Artificial Intelligence In Medicine 120 (2021) 102165

Contents lists available at ScienceDirect

Artificial Intelligence In Medicine

journal homepage: www.elsevier.com/locate/artmed

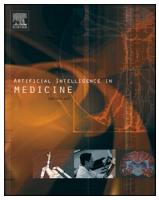

Artificial intelligence applied to support medical decisions for the automatic analysis of echocardiogram images: A systematic review

Vilson Soares de Siqueira [a,c,*], Moisés Marcos Borges [b], Rogério Gomes Furtado [b], Colandy Nunes Dourado [b], Ronaldo Martins da Costa [c]

[a] Federal Institute of Tocantins, Av. Bernado Sayão, S/N, Santa Maria, Colinas do Tocantins, TO, Brazil
[b] Diagnostic Imaging Center - CDI, Av. Portugal, 1155, St. Marista, Goiânia, GO, Brazil
[c] Federal University of Goias, Alameda Palmeiras, Quadra D, Câmpus Samambaia, Goiânia, GO, Brazil

ARTICLE INFO

Keywords:
Echocardiogram
Echocardiography
Machine Learning
Deep Learning

ABSTRACT

The echocardiogram is a test that is widely used in Heart Disease Diagnoses. However, its analysis is largely dependent on the physician's experience. In this regard, artificial intelligence has become an essential technology to assist physicians. This study is a Systematic Literature Review (SLR) of primary state-of-the-art studies that used Artificial Intelligence (AI) techniques to automate echocardiogram analyses. Searches on the leading scientific article indexing platforms using a search string returned approximately 1400 articles. After applying the inclusion and exclusion criteria, 118 articles were selected to compose the detailed SLR. This SLR presents a thorough investigation of AI applied to support medical decisions for the main types of echocardiogram (Transthoracic, Transesophageal, Doppler, Stress, and Fetal). The article's data extraction indicated that the primary research interest of the studies comprised four groups: 1) Improvement of image quality; 2) identification of the cardiac window vision plane; 3) quantification and analysis of cardiac functions, and; 4) detection and classification of cardiac diseases. The articles were categorized and grouped to show the main contributions of the literature to each type of ECHO. The results indicate that the Deep Learning (DL) methods presented the best results for the detection and segmentation of the heart walls, right and left atrium and ventricles, and classification of heart diseases using images/videos obtained by echocardiography. The models that used Convolutional Neural Network (CNN) and its variations showed the best results for all groups. The evidence produced by the results presented in the tabulation of the studies indicates that the DL contributed significantly to advances in echocardiogram automated analysis processes. Although several solutions were presented regarding the automated analysis of ECHO, this area of research still has great potential for further studies to improve the accuracy of results already known in the literature.

1. Introduction

Cardiovascular diseases have become the leading cause of death in industrialized countries [1]. In light of this scenario, researchers around the world are looking for ways to help save lives. Driven by this motivation, certain research groups have used historical data, images, and patient examination reports to develop models that use AI to predict possible implications for their clinical conditions.

One of the most common techniques for diagnosing heart disease is the Cardiac Ultrasound or Echocardiogram - ECHO. Progress in the analysis of ultrasound images has always been fundamental to advance research in image-oriented diagnostics because ultrasound provides real-time image acquisition [2]. Ultrasound is used to assess overall cardiac structures and functioning, it is minimally invasive, and does not expose the patient to radiation.

ECHO analysis is largely dependent on the physician's experience. However, AI can be used to identify, quantify, and interpret ECHO images. ML models reduce the time needed to analyze images/videos, streamlining clinical decision-making, and providing interactive feedback to train less-experienced physicians [3].

This work presents an SLR of primary studies of AI techniques applied in the automated analysis of Echocardiograms to support

* Corresponding author at: Federal Institute of Tocantins, Av. Bernado Sayão, S/N, Santa Maria, TO, Brazil.
E-mail addresses: vilsonsoares@ifto.edu.br (V.S. de Siqueira), ronaldocosta@inf.ufg.br (R.M. da Costa).
URL: http://www.ifto.edu.br (V.S. de Siqueira), http://www.cdigoias.com.br (C.N. Dourado), http://www.inf.ufg.br (R.M. da Costa).

https://doi.org/10.1016/j.artmed.2021.102165
Received 20 April 2021; Received in revised form 7 August 2021; Accepted 31 August 2021
Available online 9 September 2021

computer-oriented medical decision-making. This SLR included over 117 papers, most of them recent, covering a wide variety of applications of AI to ECHO analysis.

Although similar works are found in the literature that investigated AI application in the automated analysis of echocardiographic images, only the articles found in [4,5] addressed the SLR methodology. The first covered three echo imaging modes, which were B-mode, M-mode, and Doppler. The second covered machine learning applied to support medical decisions in Transthoracic Echocardiograms. The other articles found used the Survey or Literature Review methodologies. This SLR presents a complete survey of the advances in AI for all types of echocardiogram (Transthoracic, Transesophageal, Doppler, Stress, and Fetal).

The aim of this article was to carry out a secondary study on AI techniques used to support medical decisions and for the automation of ECHO analysis processes. The specific objectives were: to perform a search in the main scientific bases of studies on AI techniques applied to ECHO; to read the articles and create mini-abstracts of each; to group primary studies that had similar objectives; to categorize the mini-abstracts; to identify state-of-the-art whenever possible, and; to identify the challenges/limitations of using AI in this context.

The main contributions of this paper are:

- This SLR presents a thorough investigation into advances in the application of AI for automated image/video analyses of echocardiogram types (transthoracic, transesophageal, Doppler, stress, and fetal).
- The articles were grouped and categorized by ECHO type, following the steps presented by [4,5]
  1. Improvement in image quality;
  2. Identification of the cardiac window vision plane;
  3. Quantification and analysis of cardiac functions;
  4. Detection and classification of cardiac diseases.
- The AI techniques/methods used, and their respective metrics and precisions for each article presented.
- The main datasets available in the literature for use in experimental analyses identified.
- State-of-the-art for the Camus Dataset presented.
- Challenges/limitations to the research problem identified.

The remainder of this article is divided into the following sections: the SLR methodologies and protocols are presented in Section 2. The data extraction and mini-abstracts are grouped and presented in Section 3. The research questions are discussed and answered in Section 4. Finally, our conclusion is presented in Section 5.

2. Materials and methods

A systematic literature review is particularly intended to provide an impartial, objective and systematic approach to answering a research question by finding all relevant research results from primary empirical studies. In this regard, a SLR is considered a secondary study [6].

This work presents a SLR of primary studies on AI techniques applied to the automated analysis of Echocardiograms to support computer-oriented medical decision-making. The review presents the results found for the following types of echocardiogram: Transesophageal, Fetal, Doppler, Stress, and Transthoracic. The SLR was conducted according to the guidelines described by Kitchenham et al. [7] and was divided into three stages: Planning, Selection, and Critical Analysis of the results.

2.1. Planning

The planning stage was conducted as follows: 1) An exploratory analysis of the literature was carried out to define the keywords and the sources to be researched; 2) A search was performed in the main scientific bases of the health area (Pubmed). Initially, the terms *Echocardiogram OR Echocardiography* were used to search the relevant articles to find a satisfactory search string; 3) Search filters were added with the inclusion of the terms "*Machine learning OR Deep Learning*" to refine the search; 4) The full text search string was as follows: ((*Echocardiogram OR Echocardiography*) AND ("*Machine learning*" *OR* "*Deep Learning*")), Other keywords, such as "*Artificial Intelligence*", were tested, however, they did not add value to the research; 5) Finally, the articles were extracted from the following scientific bases: ACM (Association for Computing Machinery) [8]; IEEE (Institute of Electrical and Electronics Engineers) [9]; Science Direct [10]; PubMed [11]; and Web Of Science [12]. The search was restricted to articles published between January 2015 and October 5, 2020, and written in English.

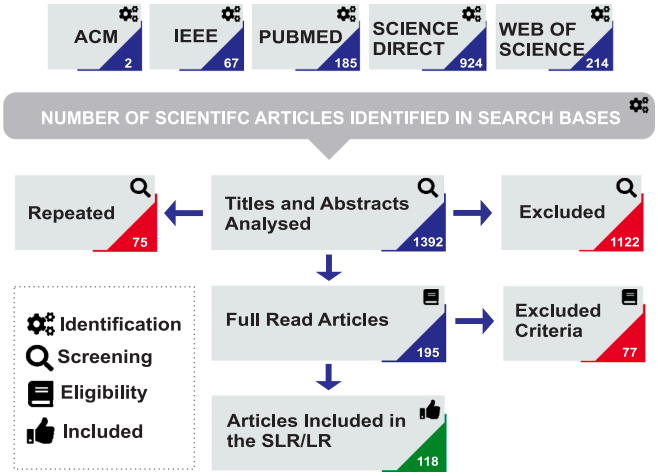

Fig. 1. The SLR article selection step.

The SLR aimed to answer the following research questions:

- Q1) In which types of echocardiogram was AI applied to support the medical decision?
- Q2) What type of echocardiogram was the most studied in research?
- Q3) What were the techniques and precision of the AI models applied?
- Q4) What were the challenges/limitations in applying AI to each type of echocardiogram?
- Q5) What techniques/methods were the most used?
- Q6) How can AI contribute to support medical decisions in analyzing echocardiogram images/videos?

2.2. Selection

In order to select the articles that comprised the SLR, the protocol followed the guidelines of Kitchenham et al. [13]. The article selection was based on the following inclusion (I) and exclusion (E) criteria:

- I1) Articles that used AI techniques for echocardiography analysis;
- I2) Articles that were complete and written in English.
- I3) Articles that presented primary studies;
- E1) Articles that did not have the type of echocardiogram exam.
- E2) Articles that did not specify the AI technique used, were incomplete, or were abstracts.
- E3) Articles that did not present the experimental results.

In Fig. 1 a summary is presented of the quantitative results returned from each scientific base using the search string mentioned in the SLR article selection step. The searches in the leading scientific bases returned a total of 1392 articles. After reading the titles and abstracts, 1122 were discarded. Thus, 270 articles remained. Among these, 75 were repeated. Therefore, 195 articles were selected for the complete

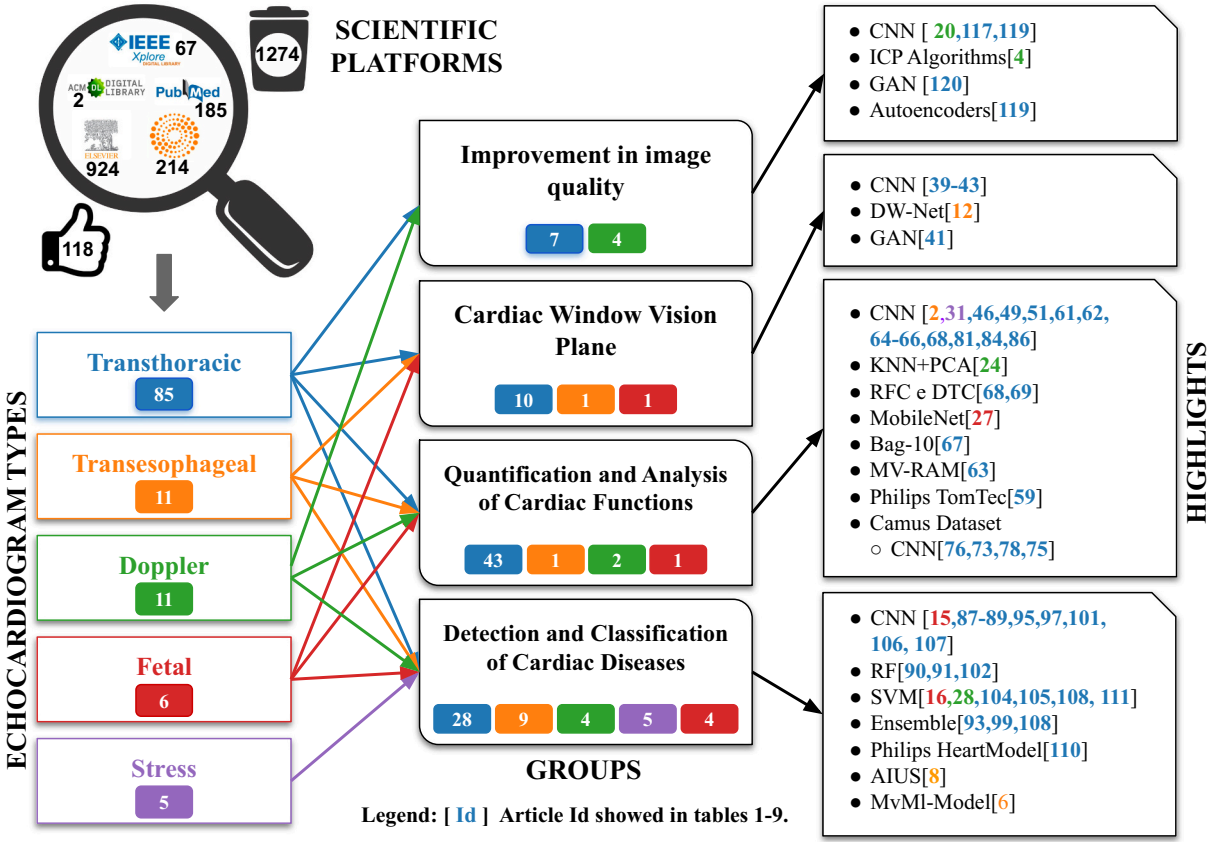

Fig. 2. Summary with SLR sequence flow and highlights.

reading and data extraction phase. After completing the full reading of the articles, 77 met the exclusion criteria (E1, E2, and E3) and were not included. Finally, 118 articles were included in the SLR.

In Section 3, the results and mini-abstracts of the articles are presented, classified by type of ECHO, and separated by problem approach.

3. Artificial intelligence applied in echocardiogram analysis

In recent years, AI has brought about significant changes in the daily lives of consumers and professionals. In the health area, AI is used to support medical decision-making in the analysis of various types of test. A common task in a doctor's routine is to analyze test images to diagnose various types of disease. In this sense, the automation of routine tasks optimizes a professional's time. Several promising solutions have been presented that cater to diverse professional specialties. Among these are the analysis of X-rays, Computed Tomography, Magnetic Resonance, Ultrasound, and others. However, some areas have evolved more than others. The main explanation for this is the number of public datasets available to study the problem and present robust solutions. Research on the application of AI techniques for the analysis of echocardiographic images has increased in recent years. However, most research used proprietary and restricted datasets, hindering reproducibility and the testing of new approaches.

Fig. 2 presents a summary of the sequence flows of the SLR development. The searches for articles were conducted in the leading scientific search platforms, they were then grouped by type of ECHO, separated into study approach categories, and lastly, a list of the main techniques was prepared.

In the article data extraction phase, ML techniques were identified that automated various stages of the echocardiogram exam. According to Zhang et al. [14], advances in computer vision may allow the construction of a fully automated and scalable analysis pipeline for the interpretation of echocardiograms, including (1) visualization identification, (2) image segmentation, (3) quantification of structure and function, and (4) detection of diseases. The articles were categorized into groups and sub-groups, and were again grouped into four categories based on the pipeline, and the extraction of the data was directed to (1) improvement in image quality; (2) identification of the cardiac window vision plane; (3) quantification and analysis of cardiac functions; and (4) detection and classification of cardiac disease. Subgroups are shown when there was more than one different subcategory belonging to a group. The mini-abstracts were ordered by year and grouped by the technique used. The articles included in the SLR were categorized by type of echocardiogram and grouped according to the above categories to facilitate analysis and understanding. This way, the reader is provided with a quick view of each sub-problem.

In the next subsections, we discuss the main advances, advantages, disadvantages, and challenges of the researchers.

3.1. Related works

Zamzmi et al. [4] carried out a systematic review to understand the existing methods for four main tasks: assessing the quality of the echo, viewing classification, limiting segmentation, and diagnosing heart disease. The review covered three ECHO image modes, which were B-mode, M-mode, and Doppler. They also discussed the challenges and limitations of current methods and outlined the most urgent directions for future research.

Siqueira et al. [5] conducted a systematic review to investigate which artificial intelligence methods were being applied in the automated analysis of transthoracic ECHO. The results directed the investigation towards three primary study groups: identification of the cardiac vision plan, analysis of cardiac functions, and detection of cardiac diseases. The review identified which ML techniques are being used to

automatically detect segmentation, and classify ECHO images.

Al'Aref et al. [15] carried out a literature review of the application of ML in cardiovascular diseases. Their studies showed that clinical ECHO algorithm efforts were directed to 4 tasks, namely: 1) Classification of visualization; 2) Image Segmentation; 3) Natural processing language; and 4) Noises in the images.

In the review by Liu et al. [16], first, they briefly introduced several popular deep learning architectures, and then fully summarized and discussed their applications for various specific tasks in ultrasound images analysis, such as classification, detection, and segmentation. Finally, the open challenges and potential trends in the future application of DL in the analysis of medical ultrasound images were discussed.

In the work by Olsen et al. [17] they presented a review article, provided an overview of ML directed to clinical analysis, and evaluated the current applications of ML in the diagnosis, classification, and prediction of heart failure.

Alsharqi et al. [18] discussed the ML subfield of AI that is relevant for image interpretation. The topics discussed were the potential of ML to improve the performance of the diagnosis of ECHO, recent applications of these methods, and future guidelines for the assisted interpretation of ECHO by AI.

Gandhi et al. [19] described the role and current use of AI automation applied to echocardiography, and discussed the potential limitations and future challenges.

Xu et al. [20] presented a review providing a contemporary overview of AI applications in cardiovascular imaging, including a critique of the strengths and potential limitations of DL approaches.

Kusunose [21] presented a review to show that the use of radiomic information in echocardiography to train DL models has a strong potential to improve clinical workflows and diagnostic accuracy.

3.2. Transesophageal echocardiogram

In Transesophageal Echocardiography (TEE), the ultrasound transducer is placed paired with the esophagus, which allows the evaluation of the heart and specific cardiac structures due to the proximity of these organs.

3.2.1. Cardiac imaging planes

Lili et al. [22] made an adaptation to the AdaBoost algorithm to detect the A4C cardiac vision plane and called it ImAdaBoost. Its accuracy was 82.84%.

3.2.2. Estimate LV basal deformation

Haukom et al. [23] trained an unsupervised CNN-based model to calculate nonlinear deformation between subsequent images in a left ventricular (LV) TEE sequence, and estimated basal deformation to monitor the patient during cardiac surgery. The difference between the model's results with an expert's annotations was 7.25% (±4.56%), on average.

3.2.3. 2D TEE aortic valve disease

Thalappillil et al. [24] evaluated an automated echocardiography software package to measure the aortic valve ring, to compare it with the computer tomography results of patients with aortic stenosis. The authors showed that there was an acceptable correlation in their hypothesis. The aortic ring measurements acquired by the software were (r = 0.84), and the computed tomography measurements were (r = 0.85).

3.2.4. 3D TEE aortic valve disease

Queirós et al. [25] presented a new algorithm for a fully automatic aortic valve (AV) segmentation of 3D TEE dataset. The algorithm was proposed and validated to quantify relevant AV measures, and proved to be robustly and accurately capable of quantifying non-aesthetic and stenotic AVs with overall viability above 90%.

3.2.5. 3D TEE mitral valve disease

Calleja et al. [26] used 3D TEE to identify specific preoperative quantitative parameters of the Mitral Valve associated with the length of the implanted mitral annuloplasty band and the performance of leaflet resection in patients with Mitral Valve Degenerative Disease undergoing repair.

Sotaquira et al. [27] presented a new algorithm for the segmentation and morphological quantification of the mitral annulus and mitral leaflets in the closed valve configuration from the RT3-D TEE volumes. After initialization, the mitral ring and mitral leaflets, as well as the coaptation line were obtained automatically.

Kagiyama et al. [28] conducted a study to investigate the effectiveness and precision of the quantification of the Mitral Valve in TEE 3D using a commercially available automated software package developed for this specific task. As a result, they observed that the automatic software significantly reduced the evaluation time compared to the manual software. The time was reduced from (770 ± 89) to (315 ± 37) seconds.

Jin et al. [29] proposed a new ML technique called Anatomical Intelligence in Ultrasound (AIUS) for 3D TEE. It semi-automatically tracked the anatomy of the ring and the Mitral leaflet for parametric analysis. The study's objectives were to examine whether AIUS was able to improve the accuracy and efficiency in locating Mitral Valve Prolapse among operators with different levels of experience. Manual segmentation by specialists did not have significantly lower sensitivity (60% vs 90%, $P < 0.001$), specificity (91% vs 97%, $P = 0.001$), and precision (83% vs 95%, $P < 0.001$) compared to experts.

Zhang et al. [30] proposed and developed a semi-automated framework that combined ML models with geometric and biomechanical image analysis models to build a specific representation of the patient's mitral valve that incorporated material properties derived from the image. They used 3D TEE images of the open and closed mitral valve.

Andreassen et al. [31] presented a fully automatic method for the segmentation of the mitral ring for 3D TEE that did not require manual entry. Each 3D recording was decomposed into a set of 2D planes, exploring the symmetry around the LV centerline. A 2D CNN was trained to predict the coordinates of the mitral annulus. The predictions of neighboring planes were then regularized, thus highlighting the continuity around the annulus. The absolute error was (8.1 ± 6.0) mm for the perimeter, and (1.6 ± 1.4) cm^2 for the area.

3.2.6. 3D TEE tricuspid valve disease

Fátima et al. [32] presented a preliminary experiment with new semi-automatic software package based on AI to analyze the 3D ETE tricuspid valve. The software offered a high correlation with surgical inspection due to its ability to analyze the valve's morphology and dynamics throughout the cardiac cycle. Besides, it allowed greater reproducibility of data analysis and reduced inter-observer variability with minimal need for manual intervention.

3.3. Fetal echocardiogram

Fetal echocardiography is a widely-used medical examination for the early diagnosis of Congenital Heart Diseases (CHD) [33].

3.3.1. Cardiac imaging planes

Xu et al. [33] proposed an end-to-end DW-Net model for the precise segmentation of seven crucial anatomical structures in the A4C view. The network comprised two components: 1) a Dilated Convolutional Chain (DCC) for “gridding issue” reduction, for the aggregation of contextual information at various scales, and the accurate localization of the cardiac chambers. 2) A W-Net to obtain more precise limits and produce refined segmentation results. The Area Under Curve (AUC) result was 0.990.

3.3.2. Cardiac function analysis

Pu et al. [34] formulated acquiring the End-Systolic (ES) and End-Diastolic (ED) of the Fetus as a classification problem. They presented a hybrid DL structure that used the class rate to locate the ES structures and ED. According to the authors, this was the first structure that used a hybrid classification structure for the detection task. The proposed architecture integrated the region of interest (ROI) extraction component based on label detection, retaining a temporal dependency module and a classification module based on a CNN transferred by domain. The authors used YOLOv3 as a ROI (MD) module to extract regions of attention to improve classification performance and determine four-chamber visualization. However, time dependency was not lost by the Frame neighbor difference when merged with the image channels. Different CNN architectures were explored, namely, Xeception, ResNet, InceptionV3, MobileNet, and NasNetmobile, and different channel fusion strategies were used: SF, DF, and MDF. The ideal DL model consisted of trained MobileNet, MDF, and RD added a transition class strategy. On average, a 94.84% accuracy rate was obtained.

Sundaresan et al. [35] developed a model using FCN to identify and segment the fetus heart. The AUC result was 0.850.

Lee and Noble [36] proposed a new space-time-based neural network model to determine the fetal heart cardiac cycle using ultrasound automatically. The model obtained an MSE precision of 0.177 when compared with Ground-Truth.

Sulas et al. [37] compared three different algorithms for the automatic detection of cardiac cycles in the fetus. Based on preliminary extraction of Pulsed-Wave Doppler (PWD) speed spectrum envelopes, the following results were obtained: model matching supervised classification of a reduced set of relevant waveform characteristics and supervised classification over the entire waveform potentially representing a cardiac cycle. A personalized data set comprising 43 traces of fetal cardiac PWD (174,319 signal segments) acquired in an A5C window was developed and used to evaluate the different algorithms. The SVM Algorithm was accurate to (98% $\pm$ 1%).

Yang et al. [38] conducted a study to segment the four cardiac chambers and the descending aorta in fetal echocardiographic images. They chose the DeepLabV3+ architecture to classify a COMMON group, and six disease groups. The names of these six groups were hypoplastic left heart syndrome (HLHS), total anomalous pulmonary venous connection (TAPVC), pulmonary atresia with intact ventricular septum (PA/IVS), endocardial cushion defect (ECD), fetal cardiac rhabdomyoma (FCR), and Ebstein's anomaly (EA). They assessed the A4C vision segmentation components and obtained the best segmentation with an average Sorensen–Dice coefficient (DICE) for Dataset1 of (0.897 $\pm$ 0.027), and of for Dataset2 (0.889 $\pm$ 0.025).

3.4. Doppler echocardiogram

According to Jahren et al. [39] Doppler spectrum recordings are often used to examine cardiac wall movements, flow patterns, and valve diseases.

3.4.1. Quality improvements in ECHO Doppler

Jahren et al. [39] presented a method based on Deep Learning to detect the diastolic end in a Doppler spectrum spectrogram. They explored the three modalities of Doppler spectrograms (continuous wave, pulsed wave, and tissue speed Doppler) to train a model that combined CNN to extract characteristics with RNN to extract temporal relations. The method obtained a detection accuracy rate of 97.7%.

Jalali et al. [40] proposed a temporal interpolation method using Splines. Comparison of the results of state-of-the-art methods proved to be promising for the improvement of 2D and 3D ECHO frame sequences. Results demonstrated that the proposed method performed interpolation more precisely and had a 10$\times$ faster processing time compared to the most recent studies to increase frame rates. They also showed that interpolation accuracy depended greatly on the initial number of frames per second and on how many frames were to be added to the original sequence. This frame rate increase was also applied to the color Doppler in both 2D and 3D ECHOs.

Zamzmi et al. [41] proposed a DL-based method to interpret ECHO DOPPLER images. The approach performed Doppler flow classification and quality assessment. They used labeled data to train models with the VGG-16 and ResNet-50 architectures. It achieved general accuracy of 91.6% and 88.9%, respectively, for flow classification and quality assessment.

Oktamuliani et al. [42] proposed a correction and smoothing method to determine the correct Nyquist limit, and to restore the average speed to the correct value on a color Doppler ultrasound.

Zhuang et al. [43] used the YOLO model to analyze cardiac fluid flow vector (MVF) mapping based on ultrasound color Doppler data. The DL YOLO model was combined with an improved block-matching algorithm for locating and tracking the myocardial wall. Thus, the azimuth speed of the myocardial wall-stains could be obtained. Moreover, they proposed using a non-linear weight function to fuse the radial velocity of blood particles and the speed of the azimuth of stains on the myocardial wall in a non-linear way. Thus, the vortex flow diagram cardiac flow area could be obtained. The best result was a metric AP30 of 90.36%.

3.4.2. Detection and classification of cardiac disease with ECHO DOPPLER

Narula et al. [44] used an ML structure that incorporated echocardiographic data to track spots and to automatically identify hypertrophic cardiomyopathy (HCM) of the physiological hypertrophy observed in athletes (ATH).

Tabassian et al. [45] analyzed the entire temporal profile of the LV segmental deformation curves and described their interrelationships to obtain more detailed information on the overall function of the LV in order to identify abnormal changes in the LV mechanics to detect myocardial infarction. They used PCA, and accuracy was 87.0%.

Heo et al. [46] compared the conventional PISA method with the clinical implications of 3D-FVCD transthoracic ECHO in real-time with color Doppler to quantify the volume and to detect mitral regurgitation. They identified that 3D-FVCD was superior to the conventional 2D techniques. Correlation was ($r = 0.94$) for 3D-FVCD and ($r = 0.87$) for 2D-PISA.

Chen et al. [47] used the Naive Bayes classifier to identify risk in patients with severe dilated cardiomyopathy (CDG) disease. The model may be used to guide risk stratification and patient management in the future. The result was a AUC of 0.877.

Kwon et al. [48] created a predictive model to identify the risk of death in patients who had a combination of coronary heart disease or heart failure for two groups of patients: Group1- Coronary Heart Disease, and Group2 - Heart Failure. They tested 10 ML models, where accuracy using DL was greater. The results were AUC of 0.958 for Group1, and AUC of 0.913 for Group2.

Vennemann et al. [49] carried out an in-vitro experiment to predict aortic valve degradation. They described how unsupervised novelty detection algorithms could be used to automate the interpretation of blood flow data to improve results through the early detection of adverse cardiovascular events without the need for repeated tests in a clinical setting. The proposal was tested in an in-vitro flow loop that simulated a failed aortic valve in a laboratory environment. Increasingly severe aortic regurgitation was deliberately introduced with tube-shaped inserts, preventing the valve's complete closure during diastole. Blood flow records from a flow meter at the ascending aorta site were analyzed using the algorithms introduced in their study. A diagnostic index was defined that reflected the severity of valve degradation. Average results of the training rate with fraction (Max and Min) support vector hyperparameters set at v = 0.01, 0.05 and 0.15 were, respectively, 0.995, 0.946 and 0.849.

3.5. Stress echocardiogram

Stress echocardiography is a well-established diagnostic tool for suspected coronary artery disease (CAD) [50].

3.5.1. Cardiac function analysis with ECHO stress

Bennasar et al. [50] used ML to predict significant CAD defined by positive stress echocardiography results in patients with chest pain, using anthropometry, cardiovascular risk factors, and medications as variables. Due to its conception, this could allow the clinical prioritization of patients with probable CAD prediction, saving doctors' time and improving the results. The best accuracy was 67.73% with the SVM algorithm.

Čelutkiene et al. [51] concluded that the combination of unique quantitative parameters in the multiparametric model for the detection of ischemia was not superior to the visual assessment during the dobutamine stress echocardiogram. The model had sensitivity and specificity of 91.6% and 86.3%, respectively, when compared to the visual access of 76.8% and 89.0%.

Omar et al. [52] proposed a fully automated image analysis framework for classifying abnormalities in movement of cardiac walls using 2D + T images. They carried out the traditional Classification with Random Forest and handmade Segmentation, and the hierarchical aggregation of Spatio-temporal information with a CNN-based approach. Accuracy was 75.4%.

Omar et al. [53] hypothesized that unsupervised cluster modeling using clinical and stress characteristics could detect heterogeneity in cardiovascular risk and the need for subsequent cardiac testing among the patients. The combined model showed better predictive capacity compared to clinical or stress models alone. The result was a AUC of 0.716.

Nogueira et al. [54] proposed a framework for analyzing datasets with complex data and used a dataset of handgrip exercises, including complete acquisitions of 10 healthy controls and five patients with ANT1 mutation (1377 cardiac cycles). The framework was based on an unsupervised formulation of multiple learning kernels used to integrate information from myocardial velocity and heart rate plots to obtain a lower-dimensional representation of the data.

The result of stress echocardiography and patient variables, including risk factors, current medication, and anthropometric variables, has not been extensively investigated [50].

3.6. Transthoracic echocardiogram

Transthoracic Echocardiogram (ETT) is the most widely used type because it is simple and less invasive and delivers good results. The transducer is used externally in the chest region at the cardiac window points of view to capture waves and check the complete functioning cycle of the heart.

3.6.1. Cardiac imaging planes

According to American Society of Echocardiography (ASE) guidelines [64], the acquisition of echocardiographic images is standardized. All transducers are marked to indicate the orientation of the cardiac vision windows. These are: Parasternal, Apical, Subcostal and Suprasternal.

Balaji et al. [55] proposed a fully automatic classification of cardiac window vision of echocardiograms. The system was built based on an ML approach with two types of feature: 1) Histogram features and 2) Statistical features. The accuracy was 87.5%.

The representations proposed by Penati et al. [56] depend on Bag-of-visual-words (BoVW), which has been used successfully by the computer vision community in visual recognition problems. An essential element of the proposed representations was sampling images with large regions, which drastically reduced the execution time of the image characterization procedure. The experimental evaluation of the proposed approach compared different image descriptors to classify four cardiac vision plans. The representations were robust for different image transformations, namely, downsampling, noise filtering, and different ML classifiers, maintaining the classification accuracy rate above 90.0%.

Eisman et al. [57] created an automated method based on rules for processing "indications" listed in Transthoracic echocardiogram reports and classified them into one of the main categories of the Echocardiography Appropriate Use Criteria (EAUC). It was developed and validated based on a reference standard established from experience by the physician. The method used was Term Frequency – Inverse Document Frequency (TF-IDF), widely used in Natural Language Processing (NLP) and Random Forest. Cohen's Kappa accuracy was (0.89 ± 0.06).

Zhu et al. [58] developed a framework with ML techniques using cardiac ultrasound guidelines to extract the standard plan and determine the appropriate usage steps for clinical 3D echocardiography exams. First, they used the Hough Forest (HF) technique for hierarchical research and to detect 3D resource points. Second, the initial plans were determined using anatomical regularities following the guideline. Finally, it used the Regression Forest technique to integrate the plan regularity constraints to apply to each plan. The proposed approach obtained the following orientation for the angle: (7.6 ± 4.3), for Distance: (2.5 ± 2.2), for precision: 80.4% and time of 0.8 s.

Khamis et al. [59] presented a classification algorithm that employed several stages in the space-time extraction approaches, with Cuboid Detector and supervised dictionary learning (LC-KSVD) to exclusively improve the automatic recognition and accuracy of Cardiac Vision Classification in echocardiograms. The recognition accuracy rates obtained were, respectively: 97.0%, 91.0%, and 97.0% for A2C, A4C, and ALA, with an average recognition rate of 95%.

Gao et al. [60] incorporated spatial and temporal information supported by video images of the cardiac movement, giving rise to two strands of the 2D CNN system. They conducted the fusion of both networks through linear integration of the class score vectors obtained from each of the two networks. The results of this architecture maintained the best classification results for eight categories of echocardiogram video views with an accuracy rate of 92.1%. At the same time, it achieved 89.5% using only a single space CNN network.

Madani et al. [61] used CNN to create a classification model to identify the type of vision of the echocardiogram exam. In their experiment, 15 types of cardiac vision windows[1] were labeled. The model's accuracy was 97.3% for 12 of these, and 91.7% for all 15. A echocardiography specialist assessed the same inputs, and the accuracy was 70.2–84.0% of correct answers. Madani et al. [62] used General Adversarial Network (GAN) and CNN for the same visions, and with Ensemble they managed to increase accuracy to 94.4%.

Ostvik et al. [63] used CNNs to create classification models to predict up to seven different cardiac window views. Among the experimental models, they proposed the CVC network. The model obtained 98.3% accuracy.

Zhang et al. [14] used CNN to automatically determine 23 types of cardiac view windows[2] of echocardiographic images. They obtained 84.0% accuracy.

3.6.2. Left ventricular volume and ejection fraction

For Asch et al. [92] the quantification of the left ventricular ejection fraction (LVEF) was performed with the manual or automatic identification of the endocardial limits. To calculate the final systolic and

[1] PSLA, SAX-MID, SAX-BASAL, A4C, A5C, A2C, A3C, SUB4C, SCVC, SUBAO, SUPAO, PW, CW, MMODE, RV-INFLOW.

[2] PLA.remote, PLA.zoom of LA, PLA, PLA.centered on LA, RV-INFLOW, PSA-APEX, PSAP, PSAM, PSA-AoV, PSAX-AoV zoom, A2C.no occlusions, A2C.ocluded LA, A2C.ocluded LV, A3C.no occlusions, A3C.ocluded LA, A3C.ocluded LV, A4c.no occlusions, A4C.ocluded LA, A4C.ocluded LV, A5C, Subcostal, Suprasternal, other.

diastolic volumes, a mathematical model was used. For Jafari et al. [70] LVEF was one of the primary measures used to assess heart functionality, and ECHO was the standard imaging modality used to measure LVEF.

Dong et al. [65] proposed a novel fully automatic method, combining the DL model and a deformable model. To target the LV endocardium, they trained CNN to generate a binary cuboid to locate the Region of Interest (ROI). Using ROI as an input, they trained a stacked Autoencoder model to infer the initial shape of the LV. Finally, they used the Snake model to infer the initial way of segmenting the LV endocardium. The correlation was $R^2 = 0.8184$.

Dong et al. [66] proposed a method combining Multi-scale Convolutional Deep Learning and Random Forest for the segmentation of the LV in 3D. The first method extracted the unlabeled data characteristics, and the second was used for training to perform the regression with the labeled data. The results R^2 for EDV, ESV and EF were 0.850, 0.871 and 0.863, respectively.

Leclerc et al. [67] conducted an experiment comparing the results of the CNN U-net model with Structured Random Forest (SRF) to segment the epicardium and endocardium in order to estimate the Ejection Fraction (EF) and Global Longitudinal Deformation (GLD) in the A2C and A4C views. Using the Sorensen-Dice index metric, the CNN U-net results were (0.896 $\pm$ 0.047) Endocardium (VE-endo) and (0.931 $\pm$ 0.028) Epicardium (VE-epi). Data from 400 patients were used.

Zyuzin et al. [68] used the CNN U-net model to segment the heart LV using echocardiogram images. The accuracy was 92.3%.

Raynald et al. [69] compared two complementary approaches to segmentation and automated the classification of LV position in 2D echocardiographic sequences. The first approach was based on extracting Handcraft features for contrast and position. The second followed the DL structure. Experiments have shown that the two approaches produce approximately identical performances in the visualization classification task (about 95% recognition rate).

Jafari et al. [70] presented a mobile app to estimate LVEF. It runs in real-time on Android mobile devices with a wired or wireless connection to a Point-of-Care Ultrasound (POCUS) cardiac device. The A2C and A4C visions were used by the pipeline to estimate the biplane EF. For this, they used a multitasking and computationally efficient Deep Fully Convolutional Network (DFCN) for simultaneous LV segmentation and detection of landmarks in these views. They integrated into the LVEF estimation pipeline. Accuracy was 92.0%.

The article by Veni et al. [71] presented a new framework that combined DL approach benefits with those of classic segmentation methods. The Fully Convolutional Network (FCN) architecture produced LV masks in a sequence of slightly different images with the same region and visualization. The result obtained using the DICE metrics was 0.90.

Dong et al. [72] proposed a new automatic method for LV Segmentation, based on FCN and the deformable model. With the method, they implemented the coarse-to-fine framework. First, they performed the fusion of a new deep network based on the transfer of learning and fusion of resources, combined with the residual modules to obtain a coarse segmentation of the LV on 3D echocardiography. Second, they proposed a geometric model initialization method for a deformable model based on the coarse segmentation results. Third, they implemented the deformable model to further optimize the segmentation results with a regularization item, avoiding leakage between the left atrium and the LV, achieving the refined LV segmentation target. Results were EDV ($r = 0.982$), ESV ($r = 0.979$) and FE ($r = 0.792$).

Ge et al. [73] proposed a model called a Paired-View LV Network (PV-LVNet). Its purpose is to automatically and directly estimate the indices of various types of VE from paired A2C + A4C echocardiographic views. Based on a newly designed Circle Network, PV-LVNet robustly located the VE and automatically cut the VE ROI from a A4C and A2C sequence. The location and image resampling module accurately and consistently estimated seven different indexes of multiple dimensions (1D, 2D, and 3D) and views (A2C, A4C, and A2C + A4C union). The accuracy using the MAE metric reached 2.85 mm, and the internal consistency for the estimation of cardiac indexes with the Cronbach α reached 0.974.

Zyuzin et al. [74] used several ML methods to identify the LV area edges in ECHO images. They treated the problem as a particular case of binary pixel classification. Of the methods, the Bag-10 complex model demonstrated the best classification result of 98.4%.

Bobkova et al. [76], carried out an initial work that was expanded by Bobkova et al. [75], where the authors defined the LV segmentation task and reduced it to the problem of classifying pixels in video frames. A pixel can belong to one of two classes (the background region or the LV region). They applied several classic ML algorithms. The best results were obtained from the Random Forest (RFC) and Decision Tree (RFC) Classifiers, both with AUC of 0.930.

Belous et al. [77] proposed the Contextual shape model (CSM) approach to automatically segment the VE, based on the Dirichlet process mixture model (DPMM) with the Chinese restaurant process (CRP). The approach classifies the LV function as Normal, Abnormal, and Mixed (Normal + Abnormal). Among the methods used, the CSM obtained an accuracy of 91.7%.

Ouzir et al. [1] proposed a Sparse Representation - Dictionary Learning (SR-DL) method that combined a specific similarity measure with spatial smoothness sparse regularizations, jointly exploring the statistical nature of the images obtained with the B-mode, and the smoothness and sparse properties of cardiac motion. The results were a CD_2 of (0.147 $\pm$ 0.088), a MI of (0.157 $\pm$ 0.091), and a SSD of (0.173 $\pm$ 0.105).

Bernier et al. [78] proposed a method for the 3D segmentation of the LV comprised of 4 stages. First, a 3D sampling of the LV cavity was made based on a Bezier coordinate system to change the input 3D image to a Bezier space. A plane corresponds an anatomically plausible 3D Euclidean bullet shape. Second, they constructed a 3D graph and assigned an energy term (based on the image gradient and a 3D probability map) to each end of the graph, some of which received infinite energy to ensure that the resulting 3D structure passed through the main anatomical points. Third, a minimal maximum flow cut procedure was performed on the energy graph to outline the endocardial surface. Fourth, the resulting surface was projected back onto the Euclidean space, where a convex locking algorithm for post-processing was applied to each short-axis slice to remove local concavities. In general, it obtained better results than state-of-the-art methods for the *SETUS echocardiographic dataset*.

Narang et al. [79] demonstrated a new algorithm called Philips HeartModel to perform the volumetric analysis and segmentation of the atrium and LV functions. Comparing the correlation between HeartModel vs. CMR for atrium and VE, respectively the results were (MaxV: 0.95, MinV: 0.90 and FF: 0.72) and (EDV: 0.97, ESV: 0.86 and EF: 0.79). In HeartModel vs. TomTec for atrium and VE, respectively the results were (MaxV: 0.90, MinV: 0.88 and FF: 0.87) and (EDV: 0.95, ESV: 0.97 and EF: 0.91). The time to generate the volume curve was reduced from (3.6 $\pm$ 0.9) minutes to (35 $\pm$ 17) seconds.

Volpato et al. [80] proposed an ML approach for 3D echocardiography that allowed automated determination of LV mass. The objective was to assess the approach accuracy, comparing it with the cardiac magnetic resonance (CMR) reference and conventional 3DE volumetric analysis. The results used the MAE metric of (126 $\pm$ 39) g.

Kusunose et al. [81] tested two types of input method for image classification and tested the accuracy of the prediction model for EF on a learning database containing erroneous images that the observers did not verify. The best CNN model rated video displayed a 98.1% overall test accuracy in the independent cohort. In the visualization classification model, 1.9% of the images were incorrectly labeled.

Moradi et al. [82] proposed a new architecture to insert all semantic prominence in the LV segmentation process in the U-Net model. The feature maps on all U-net decoder path levels were concatenated, and their depths were equalized and increased to a fixed dimension. This stack of resource maps was the input of the semantic segmentation layer.

The proposed model performance was evaluated using two sets of echocardiographic images: a public data set and a prepared data set. The proposed network produced significantly better results when compared to U-net, dilated U-net, Unet++, ACNN, SHG, and Deeplabv3 with a DICE of 0.953.

To perform segmentation of cardiac anatomy, Li et al. [83] developed a recurrent multi-view aggregation network (MV-RAN) to perform segmentation of echocardiographic sequences with the complete analysis of the cardiac cycle. The experiments used multi-centric and multi-scanner clinical data consisting of spatiotemporal data sets (2D + t). According to the authors, when compared to other state-of-the-art DL methods, the MV-RAN method achieved significantly superior results with a DICE of (0.92 ± 0.04).

Ta et al. [84] identified that motion tracking often depends on accurate myocardial segmentation, which can be challenging to obtain due to inherent ultrasound properties. To overcome this limitation, they proposed a semi-supervised collaborative learning network exploring overlapping features in motion tracking and segmentation. The network trained two branches simultaneously: one for motion tracking and the other for segmentation. Each branch learned to extract resources relevant to their respective tasks and shared them with the other. The learned movement estimates propagate manually over a segmented mask over time, which guides future segmentation forecasts. The result was a DICE of (0.87 ± 0.01).

Arafati et al. [85] presented a new generalizable and efficient fully automatic multi-label segmentation method for ECHO four-chamber views using FCNs and GANs. They claimed to be the pioneers in using GANs for pixel classification training, although they have not yet been used in cardiac imaging. Results: 92.1%, 86.3%, 89.6% and 91.4% for VE, DV, AE and AD, respectively.

Ahn et al. [86] designed a U-Net-inspired CNN that uses hand-drawn segmentation as a guide to learn the estimates of displacement between an original image and the unlabeled ground-truth displacement, minimizing the difference between a transformed source frame and an original destination frame. Then, they penalized the divergence in the displacement area in order to impose incompressibility within the LV. Finally, they demonstrated the model performance in synthetic and in vivo canine 2-D echocardiography data sets, comparing them with a non-rigid registration algorithm and a shape tracking algorithm. RMSE was Ux of (0.77 ± 0.29) and Uy of (0.80 ± 0.31) for the proposed SR Model.

Li et al. [87] proposed the Dense Pyramid and Deep Supervision Network (DPSN) model to interpret multi-vision and multicenter echocardiographic sequences. The DPSN model incorporates the advantages of a densely connected network, and the resource pyramid network and deeply supervised network help extract and merge holistic semantic information at various levels and scales. This capability gives the DPSN model prominent generalization and robustness, allowing it to produce an accurate interpretation. To reduce computational complexity and avoid frequent loss of information in temporal modeling, the DPSN model processes all frames independently (that is, without using temporal information) but can still achieve stable and consistent performance in the sequence. The results was a DICE ED of (0.945 ± 0.025) and ES of (0.925 ± 0.049) for frame segmentation, and a DICE of (0.921 ± 0.046) for sequence segmentation.

Sustersic et al. [88] used the CNN U-Net model to segment LV ECHO images. Accuracy was 83.5%.

Hu et al. [89] presented a Deep Learning method based on the Bilateral Segmentation Network (BiSeNet) for the automatic segmentation of pediatric A4C echocardiographic images. BiSeNet consists of two paths, a space path to capture low-level spatial resources and a context path to explore high-level semantic context resources. It presents a module to concatenate the learning paths. The results showed a DICE of 0.932 and 0.908, respectively, for LV and Atrium segmentation.

Dong et al. [90] proposed a new efficient method for 3D segmentation of the LV on echocardiography, which is essential for diagnosing heart disease. According to the author, the proposed method effectively overcame the challenges of 3D echocardiography: high dimensional data, complex anatomical environments, and limited annotation data. First, and for the first time, they proposed a deep atlas network, which integrated the LV atlas into the DL framework to address the LV 3D segmentation problem in echocardiography, and improved performance based on limited annotation data. Second, they proposed a new constraint of information consistency to improve the model's performance at different levels simultaneously and, finally, achieved effective optimization for 3D LV segmentation in complex anatomical environments. Results were a DICE of 0.97 and inference time of 0.02 s.

Smistad et al. [91] presented a proposal to real-time automatic EF and Foreshortening Detection. The method uses several deep learning components, such as view classification, cardiac cycle timing, segmentation and landmark extraction, to measure the amount of foreshortening, LV volume, and EF. Validation was performed with ECHO 3D to measure the effect of the foreshortening. Difference in variability for the inter-observer obtained a MAD result of 7.2%.

3.6.3. Left ventricular ejection volume and fraction using a Camus Dataset

Leclerc et al. [93], investigated a ML solution based on the Structured Random Forest algorithm to fully automate myocardial and LV segmentation in heterogeneous clinical data. With the competitive results achieved, the authors believe that supervised learning may be the key to automatic segmentation of the heart. The results for segmentation of VE were (EDV of (0.92 ± 0.03) and ESV (0.93 ± 0.04)) and Myocardium (EDV of (0.88 ± 0.08) and ESV of (0.90 ± 0.08)).

Leclerc et al. [94] assessed the extent to which state-of-the-art Deep Convolutional Neural networks (DCNN) Encoder/Decoder methods can evaluate 2D echocardiographic images, that is, segment cardiac structures and estimate clinical indexes in a single data set. They also made the database publicly available with information from 500 patients. The results show the specialized analysis of the volume of EDV and ESV. The mean correlation was 0.95 with an absolute mean error of 9.5 ml. Regarding FE-VE, the results were more in contrast with an average correlation coefficient of 0.80 and an average absolute error of 5.6%.

Leclerc et al. [95] presented a new mechanism of attention for refining the endocardium segmentation and epicardium in 2D echocardiography. The model used two U-Net networks to derive the region of interest from the image before segmentation. The model used parameterized sigmoids to perform threshold operations. The architecture was trained from end-to-end and named Refining U-Net (RU-Net). DICE results were (0.921 ± 0.054) for VE-Endo and (0.948 ± 0.006) for VE-Epi.

Smistad et al. [96] transferred learning from a trained model to segment views from A2C/A4C echocardiographic window data from 106 patients with ALAX vision in conjunction with the CAMUS Dataset, which had 500 patients with A2C/A4C views. However, the results were unsatisfactory, reducing accuracy. They thus proposed a network with A2C, A4C and ALAX Multi-view segmentation to segment the LV, Myocardium and Atrium, respectively with DICE of (0.921 ± 0.03), (0.786 ± 0.08) and (0.892 ± 0.08).

Leclerc et al. [97] presented a new multi-stage care network to improve the robustness of the segmentation of ECHO 2D LV structures. The network was built around the U-Net architecture and consisted of two stages: The first network extracted the LV region and its mask. The second network used the extracted image to segment the region. The solution's performance was assessed with the most extensive set of current open access 2D echocardiographic data, the CAMUS Dataset. The average Correlation Coefficient result was 0.96 to detect EDV and ESV, and the result for MAE was 7.6 ml. For FE, the correlation coefficient was 0.83 and 5.0% for MAE.

Amer et al. [98] proposed a new method based on Deep Learning called ResDUnet for LV segmentation and to estimate EF. The model was based on embedded U-Net with extended convolution, where residual blocks were used instead of U-net network units. Result was a DICE of

0.951 ± 0.030.

Zyuzin et al. [99] trained a model by combining the U-Net architecture with Residual Blocks, and the U-net ResNet-34 architecture obtained respective DICE results of 0.9348, 0.9459, 0.9038 for Ve-endo, VE-epi and AE.

3.6.4. Right ventricular ejection fraction and volume

Genovese et al. [100] tested the accuracy and reproducibility of a new fully automated ML-based software for 3D quantification of the right ventricular (RV) size and function. The ML-based 3DE algorithm provided accurate and completely reproducible measurements of the RV and EF volume in one-third of the patients, with no editing of the image limits. In the remaining patients, minimal and rapid editing resulted in reasonably accurate measurements with excellent reproducibility. The correlation was ($r = 0.91$) for EDV, ($r = 0.92$) for ESV, and ($r = 0.87$) for FE.

Ahmad et al. [101] compared 4 ML algorithms to identify patients with depressed RV function using 2D ECHO parameters in conjunction with clinical features. The result of the RF algorithm, using the AUC metric, was 0.86.

Beecy et al. [102] presented a new CNN model to track the tricuspid annulus on ECHO. The model was trained using 7791 image frames, and automated linear and circumferential indices quantifying annular displacement were generated. Automated indices were compared to an independent reference of cardiac magnetic resonance (CMR) defined RV dysfunction (RVEF < 50%). Automated segmentation techniques provided good diagnostic performance (AUC = 0.690–0.730) in relation to the CMR reference, compared to the conventional RV indices plane (tricuspid annular plane systolic excursion (TAPSE) and RV the systolic excursion velocity (S')), with a high negative predictive value (NPV 84%–87% vs. 83%–88%).

Bellavia et al. [103], to identify the most accurate predictors of right ventricular failure among clinical, biological, and imaging markers, assessed through agreements of different supervised ML algorithms, found that Naive Bayes obtained a AUC of 0.970.

3.6.5. Myocardial wall motion

Yuan et al. [104] created a procedure that involves a simple application of non-negative matrix factorization (NMF) to a series of frames from a single patient video. The NMF Rank-2 was performed to calculate the two final members. The final limbs are shown as intimate representations of the heart's actual morphology at the end of each phase of cardiac function. Besides, the entire time series can be represented as a linear combination of these two end-member states, thus providing a shallow dimensional representation of the heart's time dynamics.

Omar et al. [105] proposed a structure for a fully automated image analysis to classify abnormalities of the movement of the myocardial walls in 2D + T images. They showed that by pre-processing raw videos with the asymmetric characteristics method and feeding them a CNN of temporal space achieved the best results for classifying myocardial wall movement. The accuracy was 85.4%, specificity 77.6%, and sensitivity 92.8%.

Outar et al. [106] proposed a method that combines a specific similarity measure with spatial smoothness and sparse regularizations, jointly exploring the statistical nature of B-mode ECHO images, and the smoothness and sparse properties of cardiac movement. Three types of similarity measures were used: CD_2 of (0.147 ± 0.088), MI of (0.157 ± 0.091), and SSD of (0.173 ± 0.105).

Kusunose et al. [107] investigated whether DCNN could provide improved detection of regional wall movement abnormalities (RWMAs), and differentiated between groups of coronary infarction regions from conventional 2D echocardiographic images. They then compared the results of the model with cardiologists (0.97 vs. 0.95), sonographers (0.97 vs 0.95), and resident readers (0.97 vs. 0.83).

3.6.6. Heart diseases - hypertrophy in the left ventricle

Silva et al. [108] presented a CNN 3D model to classify the level of LVEF abnormality, in which LVEF was represented with the following continuous values for each class, where 1 = Unhealthy (<45%), 2 = Intermediate (45% ≥ 55%), 3 = Healthy (55% ≥ 75%), and 4 = Abnormally high (>75%). Its accuracy was 78.0%.

Madani et al. [62] used supervised and semi-supervised DL models to classify hypertrophy in Normal or Abnormal LV. For the supervised model, accuracy was 91.2% using CNN. For the semi-supervised model with only 4% of the labeled data, precision was greater than 80% using GANs.

Zhang et al. [14] used CNN for hypertrophic cardiomyopathy (CHD), pulmonary arterial hypertension (PAH), and cardiac amyloidosis (DAMC), respectively, with an accuracy of 93.0%, 85.0%, and 87.0%.

Zhong et al. [109] carried out a comparative study using different parameters obtained with ECHO 3D Speckle Tracking (Tracking Spots) of patients with Acute Myocardial Infarction (AMI). They then built a model to predict AMI risks after Percutaneous Coronary Intervention (PCI). The results showed that RF was better, with an AUC of 0.960.

Sabovcik et al. [110] evaluated several ML classifiers, using 67 routinely measured clinical, biochemical, and electrocardiographic characteristics to detect subclinical LV abnormalities as inputs, then combined them with the echocardiographic LV diastolic dysfunction (LVDD) and the LV hypertrophy (LVH). The RF model was better, with an AUC of 0.881 for LVDD and 0.785 for LVH.

Mishra et al. [111] highlighted that many individual echocardiographic variables are associated with patients with CAD. However, they have not been combined in prediction models. In this regard, they performed an analysis of an unsupervised model for a study of 1000 patients with stable CAD, with 15 TTE variables. The result using the Harrell C-index for HFI was (0.84; 95% CI, 0.81–0.87).

Kwon et al. [112] conducted a comparative performance study between the diagnosis of AI models and conventional criteria for detecting LV hypertrophy using electrocardiogram and echocardiogram. The results showed that the accuracy of the diagnosis performed by cardiologists was 85.5%, while an Ensemble Neural Network model had an accuracy of 88.8%.

Ghorbani et al. [113] used CNN in a new large data set, showing that DL applied to echocardiography can identify local cardiac structures, estimate cardiac function, and predict systemic phenotypes that modify cardiovascular risk but that are not visibly identifiable for human interpretation. The EchoNet Dynamic model accurately identified the presence of pacemaker electrodes (AUC = 0.890), enlarged left atrium (AUC = 0.860), LV hypertrophy (AUC = 0.750), end-systolic and diastolic volume VE ($R^2 = 0.74$ and $R^2 = 0.70$), and ejection fraction ($R^2 = 0.50$), and also predicted systemic age phenotypes ($R^2 = 0.46$), sex (AUC = 0.880), weight ($R^2 = 0.56$), and height ($R^2 = 0.33$). The interpretation analysis validated that EchoNet-Dynamic gave adequate attention to the main cardiac structures when performing tasks that humans explain and highlighted the regions' hypotheses that generated interest by predicting difficult systemic phenotypes for human interpretation.

Jian et al. [114] trained a CNN model to diagnose LV hypertrophy. They obtained the image ROIs using non-local means filtering (Non-local means filtering) and opening operation (Opening operation). The edge detection algorithm based on segmentation was then used. After the contour extraction, the segmentation threshold was adjusted by the OTSU algorithm. The model completed the measurement of the LV posterior wall thickness selection point. Finally, it determined whether the patient had LVH. The error was less than 15%.

Hedman et al. [115] derived groups based on hFpeF phenotype (hay groups), which were based on clinical and echocardiogram data using ML compared clinical characteristics, proteomics, and results between hay-groups. They identified six hay-groups and observed significant differences in the prevalence of concomitant atrial fibrillation (AIF), anemia, and kidney disease ($p < 0.05$). The Elastic Net model obtained

the best multi-class evaluation with AUC of 0.790.

Howard et al. [116] highlighted that current state-of-the-art methods for identifying computational visualizations involve two-dimensional CNNs. However, these merely classify individual frames of a video in isolation and ignore information that describes structure movements over the cardiac cycle. In this regard, they tested the effectiveness of the new CNN architectures, including time networks and two-stream networks, inspired by advances in recognition of human action. They reduced the error rate generated by traditional CNNs from 8.1% to 3.9%. They concluded that advances in precision may be due to the ability of these networks to track the movement of specific structures throughout the cardiac cycle, such as heart valves.

Liao et al. [117] proposed a method to model uncertainty in the context of 2D ECHO, which is a routine procedure for detecting cardiovascular disease. The quality of the ECHO image and the acquisition time depend a lot on the operator's experience level. However, the subjectivity of the observer in the assessment of the expert can affect the accuracy of the quality quantification. They then modeled intra-observer variability to assess ECHO quality as a random uncertainty modeling regression problem using categorical labels. A key feature of the project was that only a single step forward was sufficient to estimate the level of uncertainty for the network output. The model reduced the MAE from (0.11 $\pm$ 0.009) to (0.09 $\pm$ 0.008).

Kagiyama et al. [118] extracted 328 features based on myocardial texture from static ultrasound images. After exploring the myocardial texture phenotypes using unsupervised similarity networks, the global LV remodeling parameters were predicted using supervised ML models. They also developed supervised models to predict the presence of myocardial fibrosis using another cohort that underwent cardiac magnetic resonance imaging (CMR). The extraction of tissue characteristics based on texture was feasible in 97% of 534 patients. The similarity analysis between patients outlined two groups of patients based on texture characteristics: one group had more LV remodeling parameters than the other group. Besides, the group was associated with a higher incidence of cardiac deaths ($p = 0.001$) and major adverse cardiac events ($p < 0.001$).

In the research by Chandra et al. [119], a model was proposed to track the mitral leaflets for visualization with greater precision using the YOLOv3 mechanism with MobileNet backend. The approach helped ultrasonographers to identify mitral leaflets in the A4C view. They used a data set of 40 echocardiography videos from different A4C patients, data from 30 patients using 1800 images for training and 1800 images for testing. They achieved an mAP of 84.4, a detection accuracy of 98.0% for the mitral valve leaflet, and 90% for the tricuspid valve leaflet. The results were IoU of 92.3%.

Samad et al. [120] conducted a study using ML, using the Random Forest algorithm to make combinations of different input variables to predict survival after follow-up with echocardiographic analysis. The result was a AUC higher than 0.820.

Raghavendra et al. [121] presented a new computer-aided diagnostic system for the automated detection of coronary artery disease using cardiac echocardiography images obtained from A4C. The method proposed used the discrete double density wavelet and doubletree (DD-DTDWT) transformation to decompose the images into different frequency sub-bands. The method achieved an accuracy of 96.05%, a sensitivity of 96.12%, and a specificity of 96.0% for the linear discriminant classifier (LDA) using the Entropy Classification method with twelve characteristics. They also proposed a coronary artery disease risk index (CADRI) to categorize sick and normal individuals using a single value.

3.6.7. Congestive heart failure

Raghavendra et al. [122] proposed an automated screening method to classify normal echocardiographic images, congestive heart failure (CHF) images, and images affected due to dilated cardiomyopathy (DCM), using resources extracted from the image decomposed in the variational model. These features were selected using particle swarm optimization and were classified with the Support Vector Machine (SVM) using different kernel functions. Maximum average precision, sensitivity, and specificity were 99.33%, 98.66%, and 100%, respectively.

3.6.8. Mitral valve disease

Moghaddasi and Nourian [123] used the SVM, Linear Discriminant Analysis (LDA), and Template Matching (TM) techniques to classify the severity of Mitral Regurgitation (RM) based on texture descriptors. The SVM classifier using Extensive Uniform Local Binary Pattern (ELBPU) and Extensive Volume Local Binary Pattern (EVLBP) had the best accuracy with 99.52%, 99.38%, 99.31%, and 99.59%, respectively, for the detection of mild and normal RM, moderate and severe RM among the echocardiography videos. The method reached a sensitivity of 99.38% and a specificity of 99.63% in detecting RM and severity in normal individuals.

Smistad et al. [124] used the model proposed by Ostivik et al. [63] to create a program for real-time detection using streaming to detect the volume and Mitral Annular Plane Systolic Excursion (MAPSE) of the heart on echocardiograms, using a GE Vivid E95 ultrasound device. The Bland-Altmann analysis was performed for a dataset of 75 patients. The accuracy of the automatic analysis was (-13.7 ± 8.6) % for EF and (-0.9 ± 4.6) mm for MAPSE.

3.6.9. Aortic valve disease

Nizar et al. [125] used a CNN method, with the Faster R-CNN Inception V2 model to detect the aortic valve in real-time echocardiogram videos. They used a Data set with 30 videos: 23 videos with 3685 frames for training, 2 videos with 344 frames for testing, and 5 videos for validation. Accuracy was 94.9%.

Pereira et al. [126] proposed a structure that used ML methods based on DL for the fully automated detection of coarctation aortic (CoA) from 2D ultrasound clinical data acquired in the PLA, A4C, and SSNA views. In a validation set composed of 26 CoA and 64 normal patients, the algorithm reached a total error rate of 12.9% (11.5% false-negative error and 13.6% false-positive error) when combining classifier decisions into three standard echocardiographic visualization plans.

Khalil et al. [127] proposed an automatic 2D to 3D registration framework for the fusion of echocardiogram and computed tomography (CT) data, explicitly aiming to guide transcatheter aortic surgery. The technique simultaneously addressed the problems of time synchronization and spatial alignment, offering opportunities of new ways to display structural and functional information composed from intraoperative transthoracic echocardiography and preoperative CT data. The accuracy of the method was (0.81 $\pm$ 0.08) and (1.30 $\pm$ 0.13) mm in terms of data coefficient and Hausdorff distance for the PSAX vision plane of the aortic valve, while for PLAX, it was (0.79 $\pm$ 0.02) and (1.19 $\pm$ 0.11) mm.

3.6.10. Atrial disease

Otani et al. [128] conducted a study to determine the utility of the fully automated left-chamber quantification software with 3D single-beat transthoracic echocardiographic data sets in patients with Atrial Fibrillation. His comparative study proved that the automatic quantification method took significantly less time than the manual method to perform the analysis. It took 5 min for the automatic analysis, and 27 min for the manual one. Excellent correlations were found between automatic x manual quantification, for Protocol 1 (P1) of ($r =$ 0.88–0.98), and for Protocol 2 (P2) of ($r = 0.94$–0.99).

Borkar & Annadate [129] used a ROI method to extract the characteristics of the echocardiogram frame and the SVM classification to automatically detect and classify dilated cardiomyopathy (CMD), atrial septal defect (DSA), and Normal. Its accuracy was 98.3%.

Lu et al. [130] proposed a new regression method to identify abnormalities in echocardiogram B-Mode images. They used appropriate DL networks to identify Normal and Abnormal CMD cases

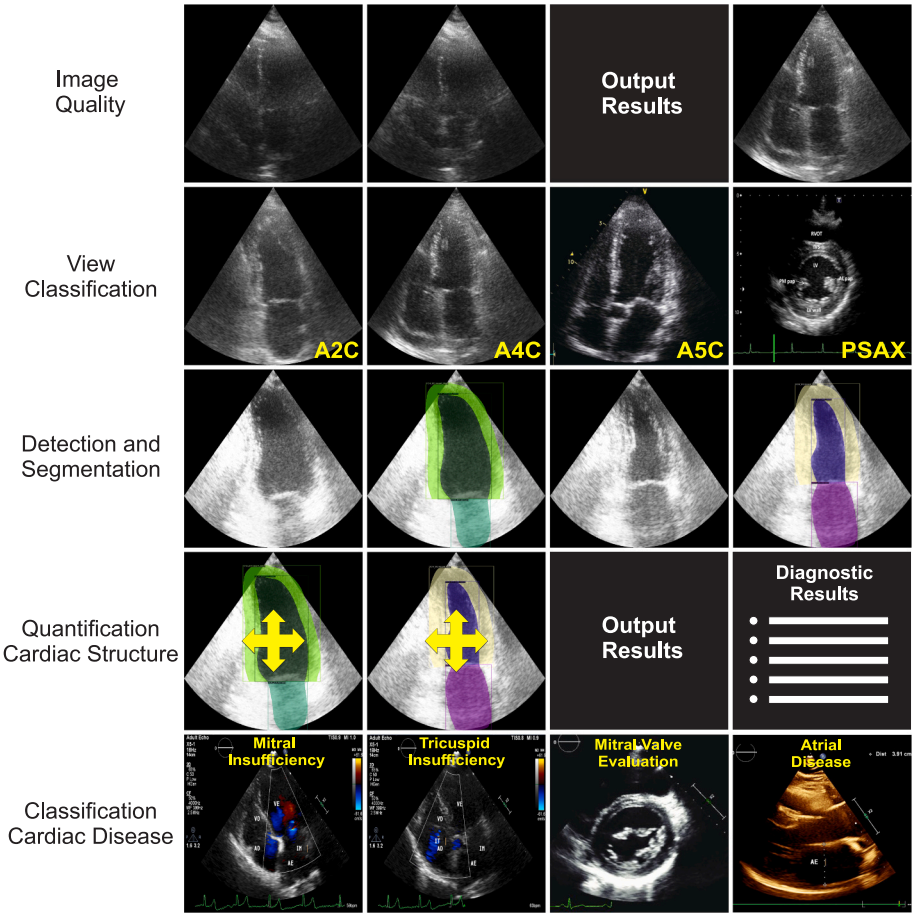

Fig. 3. Superficial overview of the steps to automate ECHO.

automatically. The precision was an AUC of 0.840.

3.6.11. *Resynchronization therapy*

Lei et al. [131] sought, for the first time, to discover new analytical approaches to improve the prediction of Cardiac Resynchronization Therapy (CRT) responses in the pre-implementation of pacemaker devices in patients. The approach used three ML algorithms (SVM, KNN, Random Subspaces) in a total of 38 resource combinations. They found that the resources combined with QRSd/RWT consistently outperformed the combinations without them. For each of the three algorithms, the combination of triple features of QRSd/RWT, LBBB, and non-ischemic cardiomyopathy repeatedly increased the classification rate by more than 8%. QRSd is Regularization Duration on QRS of the electrocardiography (ECG), RTW is Relative Wall Thickness, and LBBB is left bundle branch block. The best performance for predicting the CRT response occurred with the SVM model, which proposed real QRSd/RWT values that favored CRT responses in patients with and without LBBB. An AUC of 0.848 was obtained.

3.6.12. *Improvements in echocardiographic images*

Gifani et al. [132] performed a comprehensive comparison of algorithms for sparse recovery, where Bayesian Compressive Sensing (BCS), the Bregman iterative algorithm, and Orthogonal Matching Pursuit (OMP) were used to develop a new method. The performance of the proposed method was then evaluated and compared with other stain reduction filters. The experimental results showed that the algorithm could be used to improve edges and reduce blur.

Punithakumar et al. [133] proposed a new approach to fusing multiple 3D echocardiography images using an optical tracking system that incorporates breath-holding position tracking to infer that the heart remains in the same position during different acquisitions. The method improved the cardiac field of vision (35.4 $\pm$ 12.5%).

The study by Abdi et al. [134] aimed to reduce user variability in data acquisition by automatically computing a score for echo quality from operator feedback. For this, they developed a DL model based on CNN, trained with a large set of samples, to obtain ECHO images for A4C vision. For training, testing, and validation they used 6916 ECHO images with the final systolic segmentation annotated manually by a specialist cardiologist and received a score between (0 and 5), where "0" was not acceptable and "5" was excellent. The result using the MAE metric was (0.71 $\pm$ 0.58).

Diller et al. [135] investigated DL Autoencoder algorithms to remove noise and artifacts from transthoracic echocardiograms with A4C vision. The model sought to identify noise and artifacts, especially in patients with congenital heart disease.

Wu et al. [136] developed an algorithm using PCA and SPCA to improve the echocardiogram using a supervised noise reduction collector to incorporate context-relevant data-driven video movement instead of learning this structure directly from noisy image data.

Girum et al. [137] proposed a new efficient DL method to accurately segment image labels while generating a set of annotated data for DL methods. It involves the prediction of prior knowledge based on GANs from pseudo-contour reference points. The predicted prior knowledge (that is, the contour proposal) was refined using a CNN that took advantage of the predicted prior knowledge information and the raw input image. The poorly supervised method obtained an accuracy of (98.8 $\pm$ 0.42%).

Teng et al. [138] addressed interactive translation with limited annotations using learning transfer. First, they trained two main independent networks, the main ultrasound draft network (U2S), and the

main ultrasound draft network (S2U). U2S translation is similar to a segmentation task with region boundary inference. Therefore, the main U2S network was trained with the U-Net network in the public segmentation dataset of VOC2012. S2U aimed to recover the texture of the ultrasound. The main S2U network was a decoder network that generated ultrasound data from random inputs. After pre-training the main networks, an encoding network was connected to the main S2U network to translate the ultrasound images into sketch images. Finally, they joined the transfer of U2S and S2U learning with the CGAN Framework. The results using the DICE metric for {1,5,10} shot were, respectively, {0.902, 0.913, 0.921}.

4. Discussion

Interpretation of an echocardiogram depends on the physician's experience. For Sengupta and Adjeroh [139], recent interest in using artificial intelligence techniques may help alleviate doctor workloads, reducing repetitive and tedious tasks involved in diagnosing and analyzing data and patient images.

The SLR results indicate that the echocardiography research community is making significant progress in automated ECHO analysis. The popularization of DL and the increase in computational power in recent years has contributed significantly to improving the accuracy of the results involving computer vision. Although there have been notable developments in the use of AI in echocardiography, the area is still open. There are several research possibilities, such as: improving the accuracy of the models for the segmentation, detection, and classification of cardiac structures; proposing new methods capable of carrying out automated ECHO analyses; developing new techniques for extracting features from ECHO images; experimenting with pre-trained DL models for segmentation, detection, and classification of images available in the literature and the transfer of learning to the specific domain of ECHO; optimizing the computational time of the models to enable real-time evaluation; proposing methods capable of reducing the complexity of 3D ECHO analysis; and the use of RPA (Robotic Process Automation) in the final phase of ECHO automation, to capture text from images, apply model inference, record information in a database, among others.

In Fig. 3, a superficial view of the steps required for the automation of ECHO is presented.

4.1. Analysis of articles

The SLR article quantification obtained the following percentages: ECHO Transthoracic 72.03%, ECHO Transesophageal 9.32%, ECHO Doppler 9.32%, ECHO Fetal 5.09%, and ECHO Stress 4.24%.

4.1.1. Transesophageal

The contributions presented for 2D ETE images were: detection of the cardiac vision plane A4C [22], estimating basal deformation during the cardiac surgery procedure [23], and measurement of the aortic ring [24]. For 3D ETE were the following: segmentation of the mitral ring, detection and classification of disease in the mitral valve [26,27,28,29,30,31], the aortic valve [25], and the tricuspid valve. Most articles in table 3.2.6 made contributions to support medical decisions in diagnosing valve diseases.

4.1.2. Fetal

The ECHO Fetal is still little explored, and the approaches were as follows: detection of the cardiac vision plan [33], segmentation and detection to quantify cardiac structures [34,35,36,37], and classification of fetal heart disease [32]. All approaches used 2D images.

4.1.3. Doppler

The articles on ECHO DOPPLER adopted the following approaches: detection of the diastolic end of the Doppler spectrogram [39], 2D and 3D frame interpolation [40], improvement in the quality of the capture blood flow velocity [41,42,43], and Heart Disease Classification (hypertrophic cardiomyopathy [37], myocardial infarction [45], mitral regurgitation with 2D and 3D ECHO [46], severe dilated cardiomyopathy [47], coronary heart disease and heart failure [48], and degradation of the aortic valve).

4.1.4. Stress

For ECHO Stress, approaches were applied to detect and classify coronary artery diseases [50,51], myocardial assessment [52,54] and cardiovascular risk prediction [53].

4.1.5. Transthoracic

The results showed that 72.03% of the articles addressed ETT. Discussion was divided by approaches:

- The Cardiac Vision Image acquisition plan represented 8.40% of the articles, which presented different approaches as well as the complexity of the study, as in the article by Zhang et al. [14] that classified 23 types of views with 84.0% accuracy; In the work by Madani et al. [61] 15 types of visualization were classified, with an accuracy of 91.7%. Ostvik et al. [63] obtained an accuracy of 98.3% in 7 types of visualization. All used CNN models for classification.
- Evaluation of cardiac functions was performed by 36.13% of the articles in the SLR. Automating Left ventricular segmentation, detecting myocardial walls to estimate LV volume, and ejection fraction can reduce the manual routines of doctors allowing them to serve more patients. In the opinion of Kuronose et al. [107] echocardiographic evaluation using artificial intelligence may not be necessary for specialists; however, quantitative evaluation is nevertheless a great advantage. For Dong et al. [66] estimation of LV volumes from 3D echocardiography (3DE) is a popular clinical approach for the accurate assessment of LV function in diagnosing heart disease. On the other hand, Genovese et al. [100] emphasized that 3DE yields accurate and reproducible measurements of right ventricular (RV) size and function. However, the broad implementation of 3DE in routine clinical practice is limited because existing software packages are relatively time-consuming and require specific operator skills. In the same vein, Volpato et al. [80] pointed out that, although 3DE overcomes many limitations of 2D echocardiography, allowing direct measurements of LV mass, it is rarely used in clinical practice due to lengthy analyzes. Based on the results, it was observed that there are strong indications that the challenges posed by automated echocardiogram analyses are related to the creation of optimized models capable of providing analyses, usability, and precision in real-time.
- Cardiac pathologies represented 22.68% of articles. Cardiovascular disease is one of the most unrestrained causes of death worldwide and is considered one of the main diseases in the “middle” and “old” ages. [140]. The following studies were identified that address the tasks of classifying heart disease: Myocardial wall movements [104,52,1,107], Hypertrophy in the Left Ventricle [108,62,14,109,110,111,112,113,114,115,116,117,118,119,81,120,121], Congestive Heart Failure [122], Mitral Valve Diseases [123,124], Aortic Valve Diseases [125,126,127], Atrial Diseases [128,129,130], Cardiac Resynchronization Therapy [131].
- Procedures for improving the quality of TTE images represented 5.88% of the studies.

4.2. Answers to research questions

Q1) In which types of echocardiogram was AI applied to support the medical decision?

The review indicates that AI was applied to the following types of ECHO: ECHO Transesophageal in the subsection 3.2 and the articles are presented in Table 1; O ECHO Fetal (subsection 3.3) and Table 2; ECHO

Table 1
Articles included in SLR - transesophageal TEE.

Id	Ref.	Problem	Dim.	SPL	Vision	LT	MT	MTD/TNQ	Metrics	Precision
1	[22]	WVC	2D	–	A4C	SP	C	ImAdaboost	Acc	82.84%
2	[23]	DBasal	2D	47	A2C, A4C, PLAX	NSP	R	CNN	MAE	7.25% (±4.56%)
3	[24]	AVD	2D	47	–	–	–	Soft Approach	*r*	0.840
4	[25]	AVD	3D	40	PSAX	SP	C	ICP Algorithms	Acc	90.00%
5	[26]	MVD	3D	189	–	SP	S	MLRA	*r*	0.740
6	[27]	MVD	3D	33	A4C	SP	S	MvMl-Model	*r*	0.960
7	[28]	MVD	3D	74	–	SP	D	Soft pack MV	–	–
8	[29]	MVD	3D	6	A2C, A4C	SP	D	AIUS	Acc	95.00%
9	[30]	MVD	3D	95	–	SP	S	MB	MAE	1.86 ± 1.24
10	[31]	MVD	3D/2D	18	–	SP	R	CNN U-Net	MAE	Prm = (8.1 ± 6.0) mm, Ar = (1.6 ± 1.4) cm^2
11	[32]	TVD	3D	–	–	–	–	AutoValve Siemens	–	–

Samples (SPL), learning type (LT), supervised (SP), unsupervised (NSP), model type (MT), method/technique (MTD/TNQ) classification (C), detection (D), regression (R), segmentation (S), window view cardiac (WVC), basal deformation (DBasal), mitral valve disease (MVD), tricuspid valve disease (TVD), aortic valve disease (AVD), model biomechanical (MB), multivariate linear regression analysis (MLRA), perimeter (Prm), area (Ar), apical 4 chambers (A4C), apical 2 chambers (A2C), parasternal long axis (PLAX), parasternal short axis (PSAX), correlation (*r*), accuracy (Acc), mean absolute error (MAE).

Table 2
Articles included in SLR - fetal echocardiogram.

Id	Ref.	Problem	Dim.	SPL	Vision	LT	MT	MTD/TNQ	Metrics	Precision
12	[33]	WVC	2D	895	A4C	SP	C	DW-Net	AUC	0.990
13	[34]	CHD	2D	350	A4C, B4C, P4C	SP	C	MobileNet	Acc	94.84%
14	[35]	FCC	2D	12	A4C, LVOT, 3V	SP	C	FCN	Acc	75.40%
15	[36]	FCC	2D	91	–	SP	D	CNN/RNN	MSE	0.177
16	[37]	FCC	2D	20	A5C	SP	C	SVM	Acc	(98.0% ± 1.0%)
17	[38]	CHD	2D	91	–	SP	C	DeepLabV3+	DICE	Dataset1 = (0.0897 ± 0.027), Dataset2 = (0.889 ± 0.025)

Fetal cardiac cycle (FCC), congenital heart disease (CHD), parasternal 4 chamber (P4C), basal 4 chamber (B4C), left ventricular outflow tract view (LVOT), three vessel view (3V).

Table 3
Articles included in SLR - Doppler echocardiogram.

Id	Ref.	Problem	Dim.	SPL	Vision	LT	MT	MTD/TNQ	Metrics	Precision
18	[39]	EDDS	2D	14,861	–	SP	D	CNN/RNN	TDC	97.70%
19	[40]	InterPI	2D/3D	15	A4C	–	I	SVM	MSE	2D = 0.7536, 3D = 0.2193
20	[41]	Doppler flow	2D	100	–	SP	C	CNN	Acc	91.60%, 88.90%
21	[42]	Doppler flow	2D	–	–	–	D	Snake	–	–
22	[43]	Doppler flow	2D	30	ALA	–	C	YOLO	AP30	90.36%
23	[44]	HCM	3D	139	A4C	SP	S	Ensemble	AUC	0.795
24	[45]	FGVE	3D	600	A2C, A3C, A4C	SP	S	KNN + PCA	Acc	87.00%
25	[46]	RMi	2D/3D	152	A3C, A4C, PSLA	SP	R	CCoe	*r*	2DPISA = 0.940, 3DFVCD = 0.870
26	[47]	SDCM	2D	98	–	SP	C	Naive Bayes	AUC	0.877
27	[48]	CCD, HF	2D	27,776	–	SP	D	DL-model	AUC	Group1 = 0.958, Group2 = 0.913
28	[49]	AVD	2D	–	–	NSP	S	SVM	Score	0.995, 0.946, 0.849

End-diastolic in Doppler spectrogram (EDDS), total detection correct (TDC), image interpolation (InterPI), mitral regurgitation (RMi), LV global function (LVGF), hypertrophic cardiomyopathy (HCM), severe dilated cardiomyopathy (SDCM), coronary cardiac diseases (CCD) and heart failure (HF), aortic valve degradation (AVD), correlation coefficient (CCoe).

Table 4
Articles included in SLR - stress echocardiogram.

Id	Ref.	Problem	Dim.	SPL	Vision	LT	MT	MTD/TNQ	Metrics	Precision
29	[50]	CAD	2D	529	–	SP	C	SVM	Acc	67.63%
30	[51]	MyO	2D	151	A2C, A4C	SP	C	MLPRT	Sens/Esp	91.60%/86.30%
31	[52]	HD	2D	61	BSA, MSA, A3C, A4C	SP	C	CNN	Acc	75.40%
32	[53]	CAD	2D	445	–	NSP	C	CM	AUC	0.716
33	[54]	HD	2D	15	–	NSP	A	MKL	Cor	0.810

Coronary artery disease (CAD), heart disease (HD), cluster model (CM), myocardial ischemia (MyO), sensitivity (Sens), specificity (Esp), multiparametric (MLPRT).

Doppler (subsection 3.4), Table 3, ECHO of Stress (subsection 3.5) in Table 4 and ECHO Transthoracic (subsection 3.6), in Tables 5, 6, 7, 8, and 9.

Q2) What type of echocardiogram was the most studied in research?

The quantification of the SLR results shows that the ECHO Transthoracic corresponded to 72.03% of the articles. This percentage indicates that it was the most studied by the research community. Looking at Fig. 4, the quantitative discrepancy between ECHO types was evident. The other ECHOs represent the following percentages: ECHO Transesophageal 9.32%, ECHO Doppler 9.32%, ECHO Fetal 5.09%, and ECHO Stress 4.24%.

Q3) What were the techniques and precision of the applied AI models?

The techniques/methods, metrics and precision are available in

Table 5
Transthoracic echocardiogram - cardiac vision planning.

Id	Ref.	Dim.	SPL	Vision	LT	MT	MTD/TNQ	Metrics	Precision
34	[55]	2D	200	A2C, A4C, PSA, PLA	SP	C	BPNN, SVM	Acc	87.50%
35	[56]	2D	52	A2C, A4C, PLA, PSA-MID	SP	C	BoVW	Acc	90.00%
36	[57]	2D	30, 120	–	SP	C	TF-IDF	CK	(0.89 ± 0.6)
37	[58]	3D	–	A4C, A2C, A3C, PSAM, PSAP, PSA-APEX	SP	C	Hough forest	Acc	80.40%
38	[59]	2D	309	A2C, A4C, ALA	SP	C	LC-KSVD	Acc	95.00%
39	[60]	2D	93	A2C, A3C, A4C, A5C, PLA, PSAA, PSAM, PSAP	SP	C	CNN	Acc	92.10%
40	[61]	2D	–	Vision plan[1]	SP	C	CNN	Acc	91.70%
41	[62]	2D	–	Vision plan[1]	SP	C	CNN/GAN	Acc	91.20%/92.30%
42	[63]	2D/3D	470	A2C, A4C, ALA, PLA, PSA, SC4C, SCVC	SP	C	CNN	Acc	98.30%
43	[14]	2D	460	Vision plan[2]	SSP	C	CNN	Acc	84.00%

Acronyms of the vision columns: apical three-chamber (A3C), apical five-chamber (A5C), apical long-axis (ALA), PSA of aorta (PSAA), PSA of papillary (PSAP), PSA of mitral (PSAM), PSA of aortic valve (PSA-AoV), right ventricular inflow (RV-inflow), basal short axis (SAX-basal), short axis at mid or mitral level (SAX-mid), subcostal four-chamber (SUB4C), subcostal inferior vena cava (SCVC), subcostal/abdominal aorta (SUBAO), suprasternal aorta/aortic arch (SUPAO), pulsed-wave Doppler (PW), continuous-wave Doppler (CW), M-mode (mmode), and parasternal short-axis apex (PSA-APEX), subcostal four-chamber (SC4C) and vena cava inferior (SCVC), Cohen's Kappa (CK).
Vision Plan[1] Text Footnotes [1] and Vision Plan[2] Text Footnotes [2].

Table 6
Transthoracic echocardiogram - left ventricular volume and ejection fraction.

Id	Ref.	Problem	Dim.	SPL	Vision	LT	MT	MTD/TNQ	Metrics	Precision
44	[65]	LVEF	3D	–	–	SP	S	CNN, GVF-Snake	R^2	0.818
45	[66]	LVEF	3D	90	–	NSP	R	CDBN e RF	AUC	EDV: 0.850, ESV: 0.871, EF: 0.863
46	[67]	LVEF, DLG	2D	500	A2C, A4C	SP	S	DCNN	B-A	EF: (−13.7 ± 8.6) %, MAPSE: (−0.9 ± 4.6) mm
47	[68]	LVEF	2D	94	A4C	SP	S	CNN U-Net	Acc	92.30%
48	[69]	LVEF	2D	114	A2C, A3C, A4C	SP	S, C	SDM, CNN	μ	0.950
49	[70]	LVEF	2D	427	A2C, A4C	SP	S	DFC	Acc	92.00%
50	[71]	LVEF	2D	–	A4C	SP	S	U-Net + Hyb	Dice	0.900
51	[72]	LVEF	3D	–	–	SP	S	FCN	R	EDV = 0.982, ESV = 0.979, EF = 0.792.
52	[73]	LVEF-V	2D	50	A2C, A4C, A2C + A4C	SP	S	PV-LVNet	Cron-α	0.974
53	[74]	LVEF	2D	26	A4C	SP	S	Bag-10	Acc	98.40%
54	[75]	LVEF	2D	26	A4C	SP	S	RFC e DTC	AUC	0.930
55	[76]	LVEF	2D	26	A4C		S	RFC e DTC	AUC	0.930
56	[77]	LVEF	2D	–	A4C	SP	S, C	CSM, CRP	Acc	91.70%
57	[1]	LVEF	2D	–	A4C, PSA	SP		SR-DL	MAE	CD_2: (0.147 ± 0.088), MI: (0.157 ± 0.091), SSD: (0.173 ± 0.105)
58	[78]	LVEF	3D	75	ALA	SP	S	Graph cut	r	EDV: 0.990, ESV: 0.990, LVFE: 0.960
59	[79]	LVEF-V and LA	3D	20	A2C, A4C	–	S	Philips TomTec	r	EDV: 0.950, ESV: 0.970, EF: 0.910
60	[80]	LVEF	3D	23	A4C	SP	S	ML-Algorithms	MAE	126 ± 39 g
61	[81]	CV	2D	340	PLAX, PSAX, A2C, A3C e A4C	SP	C	CNN	Acc	98.10%
62	[82]	LVEF	2D	637	A2C, A4C	SP	R	MPF-Net	DICE	0.953
63	[83]	LVEF	2D + T	750	A2C, A3C, A4C	SP	R	MV-RAN	DICE	(0.920 ± 0.04)
64	[84]	SVE	2D + T	–	PLA, A2C, A4C	SSP	R	U-Net	DICE	(0.870 ± 0.01)
65	[85]	LVEF	2D	500	A4C	SP	S	FCN/GAN	DICE	EDV: 0.940, ESV: 0.930
66	[86]	CD	2D	340	PSAX	NSP	C	CNN	RMSE	Ux = (0.77 ± 0.29), Uy = (0.80 ± 0.31)
67	[87]	LVEF	2D	100	A2C, A3C, A4C	SP	R	DPSN	DICE	(0.921 ± 0.046)
68	[88]	LV	2D	18	A4C	SP	R	CNN U-Net	Acc	83.50%
69	[89]	LV, LA	2D	87	A4C	SP	C	BiSeNet	Dice	0.932/0.908
70	[90]	LVEF-V	3D	25	A2C, A3C, A4C	SP	R	AtlasNet	DICE	0.970
71	[91]	LVEF	2D/3D	515	A2C e A4C	SP	R	DL	MAD	7.2%

Tables 1 to 9 in the technical/methods, metrics, and precision columns. The results are presented separately by type of ECHO, identified by the column “Id” from 1 to 120.

Q4) What were the challenges/limitations in applying AI to each type of echocardiogram?

The Challenges/Limitations of AI use in the ECHO Analysis were collected from the articles and added to Table 10.

Q5) What techniques/methods were the most used?

Machine Learning techniques based on supervised learning were the most used, mainly models based on CNNs. They have good precision in the image/video detection, segmentation, and classification tasks. CNN-based models were able to detect state-of-the-art solutions to problems involving computer vision.

Q6) How can AI contribute to support medical decisions in analyzing echocardiogram images/videos?

Recent research indicates that systems that use AI have strong potential to automate the ECHO analysis process (e.g. automatic determination of the fetal cardiac cycle [2], fully automatic LV area ED/ES detection [91], quantification of MV [28], automated myocardial wall motion abnormality classification [105], automatic classification of

Table 7
Transthoracic echocardiogram - left ventricular ejection volume and fraction using a Camus Dataset.

Id	Ref.	SPL	Vision	MTD/TNQ	Metrics	Precision
72	[93]	500	A4C	STF	DICE	EDV: (0.92 ± 0.03), ESV: (0.93 ± 0.04)
73	[94]	500	A2C, A4C	U-Net 2	*r*	EDV: 0.954, ESV: 0.964, EF: 0.823
74	[95]	500	A2C, A4C	RU-Net	DICE	VE-Endo: (0.921 ± 0.054), VE-Epi; (0.948 ± 0.006%)
75	[96]	606	A2C, A4C, ALAX	U-Net	DICE	EDV: (0.921 ± 0.03), ESV: (0.786 ± 0.08), EF: (0.892 ± 0.08)
76	[97]	500	A2C, A4C	LU-Net	*r*	EDV: 0.96, EsV: 0.83
77	[98]	500	A2C, A4C	ResDUnet	DICE	EF: 0.951 ± 0.030
78	[99]	500	A2C, A4C	U-Net ResNet	DICE	EDV: 0.9348, ESV: 0.9459, EF: 0.9038

Table 8
Transthoracic echocardiogram - right ventricular ejection fraction and volume and myocardial wall motion.

Id	Ref.	Problem	Dim.	SPL	Vision	LT	MT	MTD/TNQ	Metrics	Precision
Right ventricular ejection fraction and volume (3.6.4) and myocardial wall motion (3.6.5)										
79	[100]	RVEF-V	3D	55	A4C	SP	S	ML-Algorithms	r	EDV: 0.91, ESV: 0.92, EF: 0.87
80	[101]	RV	2D	155	A4C, PLA, PSA, RVI	SP	C	RF	AUC	0.860
81	[102]	TAPSE	2D	101	–	SP	S	CNN	AUC	0.840, 0.870
82	[103]	RVF	2D	74	A4C	SP	C	Naive Bayes	AUC	0.970
83	[104]	EDS	2D	99	A2C, A4C, PLA, PSA	–	S	NMF	r	0.9196
84	[105]	MPC	2D + T	–	A4C	SP	C	CNN	Acc	85.4%
85	[106]	LVEF	2D	3469	A4C, PLA	SP	R	DenseNet + 2-GRU + L_{ge}	μ	ED: (0.20 ± 0.67), ES: (1.43 ± 1.30)
86	[107]	ARMPC	2D	400	–	SP	C	DCNN	Acc	91.7%

RV inflow (RVI), right ventricular failure (RVF), end diastolic and systolic (EDS).

Table 9
Transthoracic echocardiogram - heart diseases.

Id	Ref.	Problem	Dim.	SPL	Vision	LT	MT	MTD/TNQ	Metrics	Precision
Hypertrophy in the left ventricle (3.6.6), congestive heart failure (3.6.6) and mitral valve disease (3.6.8)										
87	[108]	LVEF	3D	30	A4C	SP	C	3D-CNN	Acc	78.0%
88	[62]	LVH	2D	–	Vision plan[1]	SSP	C	CNN/GAN	Acc	91.2%/92.3%
89	[14]	DCH, HAP, DAMC	2D	460	Vision plan[2]	SP	C	CNN	Acc	DCH: 93.0%, HAP: 85.0%, DAMC: 87.0%
90	[109]	IAM	3D	135	A4C	SP	C	RF	AUC	0.960
91	[110]	LVVDD, LVH	3D	1407	PLAX, A2C, A4C	SP	C	RF	AUC	LVDD = 0.881, LVH = 0.783
92	[111]	HFI	2D	1000	PSA, A2C, A4C	NSP	S	MLA	*c–St*	(0.84; 95% CI, 0.81–0.87)
93	[112]	LVH	–	21,286	–	SP	S	Ensemble	Acc	88.8%
94	[113]	CD	–	3312	A4C	SP	S	EchoNet	–	–
95	[114]	LVH	2D	50	–	SSP	S	CNN	MAE	15%
96	[115]	DC	–	–	–	SP	R	ElasticNet	AUC	0.790
97	[116]	WVP	2D	50	–	SP	R	CNN	CK	0.947
98	[117]	–	2D	3157	14 vision plan	SP	R	DenseNet	MAE	(0.09 ± 0.008)
99	[118]	IAM	2D	405	PLA	SSP	C	Ensemble	AUC	0.830
100	[119]	DVM	2D	40	A4C	SP	R	MobileNet	Acc	98.0%
101	[81]	–	2D	340	A2C, A3C, A4C, PLA, PSA	SP	C	CNN	Acc	98.1%
102	[120]	DC	2D	516	–	SP	C	RF	AUC	0.820
103	[121]	DCC	2D	95	A4C	SP	C	LDA	Acc	96.05%
104	[122]	DCM	2D	100	A4C	SP	C	PSO e SVM	Acc	99.33%
105	[123]	RMi	2D	139	A2C, A4C	SP	C	SVM, LDA	Esp/Sens	99.38%/99.63%
106	[124]	LVEF, MAPSE	2D	75	A2C, A4C	SP	S	DCNN	*r*	LVEF: (−13.7 ± 8.6) %, MAPSE: (−0.9 ± 4.6) mm
Aortic valve disease (3.6.9), atrial disease (3.6.10), resynchronization therapy (3.6.11) and image improvements (3.6.12)										
107	[125]	DAA	2D	30	PSA	SP	D	Faster R-CNN	Acc	94.9%
108	[126]	CoA	2D	64	A4C, PSA, SSNA	SP	C	SVM-Ensemble	*r*	0.129
109	[127]	DAA	2D/3D	10	PLA, PSA	SP	–	Framework	HD	Sax: 0.81, Plax: 0.79
110	[128]	FA	3D	88	A2C, A3C e A4C	SP	S	Philips HeartModel	*r*	P1: (0.88–0.98), P2: (0.94–0.99)
111	[129]	CMD, DSA	2D	–	–	SP	S, C	SVM	Acc	98.3%
112	[130]	LVEF	2D		A2C, A4C, PLA	SP	R	MP-DL	AUC	0.840
113	[131]	TRC	2D	184	A2C, A4C, PLA	SP	R	SVM	AUC	0.848
114	[132]	–	2D	17	A2C, A4C	–	–	BCS, BIA, OMP	RMSE-MAE	(4.58–0.99), (7.81–1.21), (8.38–0.97)
115	[133]	–	3D	6	P/A	–	–	WaveF	STD	(35,4 ± 12,5%)
116	[134]	–	2D	–	A4C	SP	C	PSO + DCNN	MAE	(0.71 ± 0.58)
117	[135]	–	2D	152	A4C	SP	–	CNN, AE	STD	(1.5518 ± 0.5904)
118	[136]	–	2D	10	–	SP	C	SMD	MSSIM	0.815
119	[137]	HVE	2D	595	–	SSP	S	CNN	Acc	(98.8 ± 0.42) %
120	[138]	–	2D	5152	–	SP	R	GAN	DICE	(1, 5, 10) shot: (0.902, 0.913, 0.921)

Suprasternal notch axis (SSNA), supervised manifold denoising (SMD), mean structural similarity (MSSIM), *c* statistic (*c–St*), AutoEnconders (AE), parasternal and apical (P/A), wavelet fusion (WaveF), Bayesian Compressive Sensing (BCS), Bregman iterative algorithm (BIA).
Vision Plan[1] Text Footnotes [1] and Vision Plan[2] Text Footnotes [2].

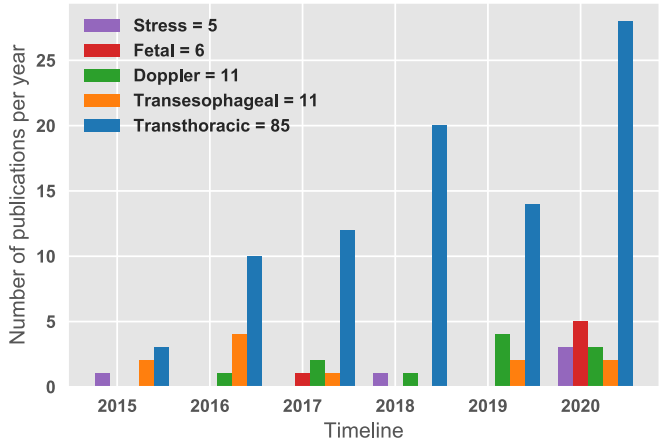

Fig. 4. Publications timelines and quantity of articles, by type of ECHO.

echocardiogram views [59], and others). Researchers are exploring several existing pre-trained DL models for other problem domains and are using transfer of learning to adapt the model to the specific ECHO domain. Automating ECHO is a challenging task. However, several applications covering specific problems and mono-tasks have been presented in the literature, offering reasonable solutions. According to the SLR articles, the main contributions were the classification of vision acquisition from cardiac windows and the identification of systolic and diastolic endings to estimate the left ventricular ejection fraction. The cardiac movement assessment allowed the assessment of cardiac functions, myocardial thickness, valve function, and cardiac contraction.

4.3. Study limitations

Our work has certain limitations. We only included papers published from January 2015 to October 2020 which are indexed in the main search platforms for scientific articles shown in the subsection 2.1. This work focused on primary studies that applied AI to automate computer-aided diagnosis processes related to ECHO. It was only possible to present the state-of-the-art for articles that used the CAMUS Dataset.

We identified that the main limitation of the area was the lack of public datasets. Most experimental studies use private datasets, so the experiments were not replicable and thus cannot be compared with other methods, making it impossible to evaluate the state-of-the-art results. The key to creating accurate models for inference in clinical practice is building a dataset from the complete RAW files that is large enough so that it can be used in the training and validation steps. The files must have the annotations of the measurements of the cardiac structures, and the measurements must be associated with the pixels for 2D evaluation and the voxels for 3D evaluation for each image/video extracted from the ultrasound equipment during the ECHO performance. Also to be highlighted is that the dataset must contain samples obtained from multiple ultrasound equipment vendors, considering that image visualization varies for each type of equipment.

Table 10
Challenges/limitations of AI use in ECHO analyses.

Challenges/limitations
• Collaboration between a computer scientist and doctors to identify the most relevant problems to be solved.
• Lack of availability of large public datasets for all types of ECHO.
• A large amount of data is required to train the DL models.
• Notes on a large amount of annotated data are required for supervised training.
• The use small datasets with supervised learning can lead to faulty assessment decisions.
• Data acquisition is generally not structured.
• Problems with efficiency and incorrect diagnoses can occur at all stages of the image analysis chain.
• Possibility of predicting wrong results.
• Models are sensitive to noisy images, and artifacts cause poor performance in model training.
• Subject to coding errors and incomplete capture of the number and severity of comorbidities.
• Problem regarding portability of the ultrasound to perform the ECHO.
• Complexity and cost, lack of common sense, assurance of patient data privacy.
• Lack of standardization of methods to ensure patient privacy.
• Ethical problems: integrity, telling the truth, doing good and avoiding evil, altruism, and humanism.
• Most experiments do not consider cohorts with data from multi-center equipment to train models.
• The quality of the model depends on the quality of the image acquisition.
• CNNs still take a long time to evaluate multiple views of ECHO.
• Model uses black box, so it does not allow humans to directly distinguish what happens to any entry.
• Lack of consensus regarding the shape of the mitral valve to estimate the effective orifice area.
• Access to fetus cardiac functions is still challenging due to its small size.

5. Conclusion

The aim of this SLR was to conduct a thorough analysis of the research advances related to the use of AI in automated echocardiogram analyses. The results are presented according to the types of ECHO: Transesophageal, Fetal, Doppler, Stress, and Transthoracic. The articles were grouped by ECHO type, with the presentation of mini-abstracts and results in Tables 1, 2, 3, 4 and Tables 6, 7, 8, and 9.

Future research efforts should aim to improve the accuracy of existing models in identifying, segmenting, and quantifying cardiac functions, classifying heart disease, and dealing with the scarcity of public datasets. Prospective studies should be well-designed and reported, especially with analyses of state-of-the-art ultrasound images. Studies should use ultrasound images from multiple vendors to ensure that the studies provide sufficiently accurate estimates for analyzing images/videos obtained using various brands and models of ultrasound equipment.

Deep Learning methods can be the key to full echocardiogram analysis automation. The results presented in this SLR show that, in the last 6 years, there have been significant advances in: (I) identification of the windows of cardiac vision plane; (II) identification, segmentation, and quantification of cardiac functions; (III) classification of heart disease; and (IV) image quality improvement.

Therefore, it is possible to conclude that this research topic still requires optimized software that can be used in real-time. It is noteworthy that this research area is open, offering many research opportunities. Therefore, it deserves the attention of researchers aiming to continuously improve ECHO quality in order to provide better results for patients, and to support doctors in their diagnoses.

Declaration of competing interest

The authors declare that they have no known competing financial interests or personal relationships that could have appeared to influence the work reported in this paper.

Acknowledgement

This document is the result of a research project funded by the Pro-Qualifier Program, the Federal Institute of Tocantins, and conducted at the Institute of Informatics of the Federal University of Goiás, in partnership with the Center for Diagnostic Imaging - CDI, Goiânia.

References

[1] Ouzir N, Basarab A, Liebgott H, Harbaoui B, Tourneret J-Y. Motion estimation in echocardiography using sparse representation and dictionary learning. IEEE Trans Image Process 2017;27(1):64–77.
[2] Noble JA. Reflections on ultrasound image analysis. 2016.

[3] Alsharqi M, Upton R, Mumith A, Leeson P. Artificial intelligence: a new clinical support tool for stress echocardiography. 2018.

[4] Zamzmi G, Hsu L-Y, Li W, Sachdev V, Antani S. Harnessing machine intelligence in automatic echocardiogram analysis: current status, limitations, and future directions. IEEE Rev Biomed Eng 2020;14:181–203. https://doi.org/10.1109/RBME.2020.2988295.

[5] de Siqueira VS, Castro Rodrigues D de, Dourado CN, Borges MM, Furtado RG, Delfino HP, et al. Machine learning applied to support medical decision in transthoracic echocardiogram exams: a systematic review. In: 2020 IEEE 44th annual computers, software, and applications conference (COMPSAC). IEEE; 2020. p. 400–7.

[6] Budgen D, Turner M, Brereton P, Kitchenham BA. Using mapping studies in software engineering. In: PPIG. vol. 8; 2008. p. 195–204.

[7] Kitchenham B, Charters S. Guidelines for performing systematic literature reviews in software engineering. 2007.

[8] Acm. acm digital library [online], in: Available: https://dl.acm.org/search/advanced; 2020, Oct.

[9] Ieee. ieee xplore digital library [online], in: Available: http://ieeexplore.ieee.org/Xplore/home.jsp; 2020, Oct.

[10] Science direct. Science Direct - Elsevier [online], in: Available: https://www.sciencedirect.com/search/advanced; 2020, Oct.

[11] Pubmed. home - pubmed - ncbi [online], in: Available: https://ieeexplore.ieee.org/search/advanced; 2020, Oct.

[12] Web of science. Web of science [online]. in: Available: https://apps.webofknowledge.com/; 2020, Oct.

[13] Kitchenham B. Procedures for performing systematic reviews. Keele, UK, Keele Univ. 2004;33(2004):1–26.

[14] Zhang J, Gajjala S, Agrawal P, Tison GH, Hallock LA, Beussink-Nelson L, et al. Fully automated echocardiogram interpretation in clinical practice: feasibility and diagnostic accuracy. Circulation 2018;138(16):1623–35.

[15] Al'Aref SJ, Anchouche K, Singh G, Slomka PJ, Kolli KK, Kumar A, et al. Clinical applications of machine learning in cardiovascular disease and its relevance to cardiac imaging. Eur Heart J 2018;40(24):1975–86.

[16] Liu S, Wang Y, Yang X, Lei B, Liu L, Li SX, et al. Deep learning in medical ultrasound analysis: a review. Engineering 2019;5(2):261–75. https://doi.org/10.1016/j.eng.2018.11.020.

[17] Olsen CR, Mentz RJ, Anstrom KJ, Page D, Patel PA. Clinical applications of machine learning in the diagnosis, classification, and prediction of heart failure. Am Heart J 2020;229:1–17. https://doi.org/10.1016/j.ahj.2020.07.009.

[18] Alsharqi M, Woodward W, Mumith J, Markham D, Upton R, Leeson P. Artificial intelligence and echocardiography. Echo Res Pract 2018;5(4):R115–25.

[19] Gandhi S, Mosleh W, Shen J, Chow C-M. Automation, machine learning, and artificial intelligence in echocardiography: a brave new world. Echocardiography 2018;35(9):1402–18.

[20] Xu B, Kocyigit D, Grimm R, Griffin BP, Cheng F. Applications of artificial intelligence in multimodality cardiovascular imaging: a state-of-the-art review. Prog Cardiovasc Dis 2020;63(3):367–76. https://doi.org/10.1016/j.pcad.2020.03.003.

[21] Kusunose K. Radiomics in echocardiography: deep learning and echocardiographic analysis. Curr Cardiol Rep 2020;22(9):1–6.

[22] Lili W, Zhongliang F, Pan T. Four-chamber plane detection in cardiac ultrasound images based on improved imbalanced adaboost algorithm. In: 2016 IEEE international conference on cloud computing and big data analysis (ICCCBDA). IEEE; 2016. p. 299–303.

[23] Haukom T, Berg EAR, Aakhus S, Kiss GH. Basal strain estimation in transesophageal echocardiography (tee) using deep learning based unsupervised deformable image registration. In: 2019 IEEE international Ultrasonics symposium (IUS). IEEE; 2019. p. 1421–4.

[24] Thalappillil R, Datta P, Datta S, Zhan Y, Wells S, Mahmood F, et al. Artificial intelligence for the measurement of the aortic valve annulus. J Cardiothorac Vasc Anesth 2020;34(1):65–71.

[25] Queirós S, Papachristidis A, Morais P, Theodoropoulos KC, Fonseca JC, Monaghan MJ, et al. Fully automatic 3-d-tee segmentation for the planning of transcatheter aortic valve implantation. IEEE Trans Biomed Eng 2016;64(8):1711–20.

[26] Calleja A, Poulin F, Woo A, Meineri M, Jedrzkiewicz S, Vannan MA, et al. Quantitative modeling of the mitral valve by three-dimensional transesophageal echocardiography in patients undergoing mitral valve repair: correlation with intraoperative surgical technique. J Am Soc Echocardiogr 2015;28(9):1083–92.

[27] Sotaquira M, Pepi M, Fusini L, Maffessanti F, Lang RM, Caiani EG. Semi-automated segmentation and quantification of mitral annulus and leaflets from transesophageal 3-d echocardiographic images. Ultrasound Med Biol 2015;41(1):251–67.

[28] Kagiyama N, Toki M, Hara M, Fukuda S, Aritaka S, Miki T, et al. Efficacy and accuracy of novel automated mitral valve quantification: three-dimensional transesophageal echocardiographic study. Echocardiography 2016;33(5):756–63.

[29] Jin C-N, Salgo IS, Schneider RJ, Kam KK-H, Chi W-K, So C-Y, et al. Using anatomic intelligence to localize mitral valve prolapse on three-dimensional echocardiography. J Am Soc Echocardiogr 2016;29(10):938–45.

[30] Zhang F, Kanik J, Mansi T, Voigt I, Sharma P, Ionasec RI, et al. Towards patient-specific modeling of mitral valve repair: 3d transesophageal echocardiography-derived parameter estimation. Med Image Anal 2017;35:599–609.

[31] Andreassen BS, Veronesi F, Gerard O, Solberg AHS, Samset E. Mitral annulus segmentation using deep learning in 3-d transesophageal echocardiography. IEEE J Biomed Health Inform 2019;24(4):994–1003.

[32] Fatima H, Mahmood F, Sehgal S, Belani K, Sharkey A, Chaudhary O, et al. Artificial intelligence for dynamic echocardiographic tricuspid valve analysis: a new tool in echocardiography. J Cardiothorac Vasc Anesth 2020;34(10):2703–6. https://doi.org/10.1053/j.jvca.2020.04.056.

[33] Xu L, Liu M, Shen Z, Wang H, Liu X, Wang X, et al. Dw-net: a cascaded convolutional neural network for apical four-chamber view segmentation in fetal echocardiography. Comput Med Imaging Graph 2020;80:101690.

[34] Pu B, Zhu N, Li K, Li S. Fetal cardiac cycle detection in multi-resource echocardiograms using hybrid classification framework. Future Gen Comput Syst 2020;115:825–36. https://doi.org/10.1016/j.future.2020.09.014.

[35] Sundaresan V, Bridge CP, Ioannou C, Noble JA. Automated characterization of the fetal heart in ultrasound images using fully convolutional neural networks. In: 2017 IEEE 14th international symposium on biomedical imaging (ISBI 2017). IEEE; 2017. p. 671–4.

[36] Lee LH, Noble JA. Automatic determination of the fetal cardiac cycle in ultrasound using spatio-temporal neural networks. In: 2020 IEEE 17th international symposium on biomedical imaging (ISBI). IEEE; 2020. p. 1937–40.

[37] Sulas E, Urru M, Tumbarello R, Raffo L, Pani D. Automatic detection of complete and measurable cardiac cycles in antenatal pulsed-wave doppler signals. Comput Methods Programs Biomed 2020;190:105336.

[38] Yang T, Han J, Zhu H, Li T, Liu X, Gu X, et al. Segmentation of five components in four chamber view of fetal echocardiography. In: 2020 IEEE 17th international symposium on biomedical imaging (ISBI). IEEE; 2020. p. 1962–5.

[39] Jahren TS, Steen EN, Aase SA, Solberg AHS. Estimation of end-diastole in cardiac spectral doppler using deep learning. IEEE Trans Ultrason Ferroelectr Freq Control 2020;67(12):2605–14. https://doi.org/10.1109/TUFFC.2020.2995118.

[40] Jalali M, Behnam H, Davoodi F, Shojaeifard M. Temporal super-resolution of 2d/3d echocardiography using cubic b-spline interpolation. Biomed Signal Process Control 2020;58:101868.

[41] Zamzmi G, Hsu L-Y, Li W, Sachdev V, Antani S. Echo doppler flow classification and goodness assessment with convolutional neural networks. In: 2019 18th IEEE international conference on machine learning and applications (ICMLA). IEEE; 2019. p. 1744–9.

[42] Oktamuliani S, Hasegawa K, Saijo Y. Correction of aliasing in color doppler echocardiography based on image processing technique in echodynamography. In: Proceedings of the 3rd international conference on biomedical signal and image processing. ACM; 2018. p. 1–5.

[43] Zhuang Z, Liu G, Ding W, Raj ANJ, Qiu S, Guo J, et al. Cardiac vfm visualization and analysis based on yolo deep learning model and modified 2d continuity equation. Comput Med Imaging Graph 2020;82:1–12. https://doi.org/10.1016/j.compmedimag.2020.101732. 101732.

[44] Narula S, Shameer K, Omar AMS, Dudley JT, Sengupta PP. Machine-learning algorithms to automate morphological and functional assessments in 2d echocardiography. J Am Coll Cardiol 2016;68(21):2287–95.

[45] Tabassian M, Alessandrini M, Herbots L, Mirea O, Pagourelias ED, Jasaityte R, et al. Machine learning of the spatio-temporal characteristics of echocardiographic deformation curves for infarct classification. Int J Cardiovasc Imaging 2017;33(8):1159–67.

[46] Heo R, Son J-W, Hartaigh B ó, Chang H-J, Kim Y-J, Datta S, et al. Clinical implications of three-dimensional real-time color doppler transthoracic echocardiography in quantifying mitral regurgitation: a comparison with conventional two-dimensional methods. J Am Soc Echocardiogr 2017;30(4):393–403.

[47] Chen R, Lu A, Wang J, Ma X, Zhao L, Wu W, et al. Using machine learning to predict one-year cardiovascular events in patients with severe dilated cardiomyopathy. Eur J Radiol 2019;117:178–83. https://doi.org/10.1016/j.ejrad.2019.06.004.

[48] Kwon J-m, Kim K-H, Jeon K-H, Park J. Deep learning for predicting in-hospital mortality among heart disease patients based on echocardiography. Echocardiography 2019;36(2):213–8.

[49] Vennemann B, Obrist D, Rösgen T. Automated diagnosis of heart valve degradation using novelty detection algorithms and machine learning. PloS One 2019;14(9):e0222983.

[50] Bennasar M, Banks D, Price BA, Kardos A. Minimal patient clinical variables to accurately predict stress echocardiography outcome: validation study using machine learning techniques. JMIR Cardio 2020;4(1):e16975.

[51] Čelutkienė J, Burneikaitė G, Petkevičius L, Balkevičienė L, Laucevičius A. Combination of single quantitative parameters into multiparametric model for ischemia detection is not superior to visual assessment during dobutamine stress echocardiography. Cardiovasc Ultrasound 2015;14(1):13.

[52] Omar HA, Domingos JS, Patra A, Upton R, Leeson P, Noble JA. Quantification of cardiac bull's-eye map based on principal strain analysis for myocardial wall motion assessment in stress echocardiography. In: 2018 IEEE 15th international symposium on biomedical imaging (ISBI 2018). IEEE; 2018. p. 1195–8.

[53] Omar AMS, Ramirez R, Haddadin F, Sabharwal B, Khandaker M, Patel Y, et al. Unsupervised clustering for phenotypic stratification of clinical, demographic, and stress attributes of cardiac risk in patients with nonischemic exercise stress echocardiography. Echocardiography 2020;37(4):505–19.

[54] Nogueira M, Craene M De, Sanchez-Martinez S, Chowdhury D, Bijnens B, Piella G. Analysis of nonstandardized stress echocardiography sequences using multiview dimensionality reduction. Med Image Anal 2020;60:101594.

[55] Balaji G, Subashini T, Chidambaram N. Automatic classification of cardiac views in echocardiogram using histogram and statistical features. Proc Comput Sci 2015;46:1569–76.

[56] Penatti OA, O. Werneck Rd, de Almeida WR, Stein BV, Pazinato DV, Júnior PRM, et al. Mid-level image representations for real-time heart view plane classification of echocardiograms. Comput Biol Med 2015;66:66–81.

[57] Eisman AS, Weiner RB, Chen ES, Stey PC, Wadhera RK, Kithcart AP, et al. An automated system for categorizing transthoracic echocardiography indications according to the echocardiography appropriate use criteria. In: AMIA annual symposium proceedings. vol. 2017. American Medical Informatics Association; 2017. p. 670.

[58] Zhu P, Li Z. Guideline-based learning for standard plane extraction in 3-d echocardiography. J Med Imaging 2018;5(4):044503.

[59] Khamis H, Zurakhov G, Azar V, Raz A, Friedman Z, Adam D. Automatic apical view classification of echocardiograms using a discriminative learning dictionary. Med Image Anal 2017;36:15–21.

[60] Gao X, Li W, Loomes M, Wang L. A fused deep learning architecture for viewpoint classification of echocardiography. Inform Fusion 2017;36:103–13.

[61] Madani A, Arnaout R, Mofrad M, Arnaout R. Fast and accurate view classification of echocardiograms using deep learning. NPJ Digit Med 2018;1(1):6.

[62] Madani A, Ong JR, Tibrewal A, Mofrad MR. Deep echocardiography: data-efficient supervised and semi-supervised deep learning towards automated diagnosis of cardiac disease. npj Digit Med 2018;1(1):59.

[63] Østvik A, Smistad E, Aase SA, Haugen BO, Lovstakken L. Real-time standard view classification in transthoracic echocardiography using convolutional neural networks. Ultrasound Med Biol 2019;45(2):374–84.

[64] Mitchell C, Rahko PS, Blauwet LA, Canaday B, Finstuen JA, Foster MC, et al. Guidelines for performing a comprehensive transthoracic echocardiographic examination in adults: recommendations from the american society of echocardiography. J Am Soc Echocardiogr 2019;32(1):1–64.

[65] Dong S, Luo G, Sun G, Wang K, Zhang H. A left ventricular segmentation method on 3d echocardiography using deep learning and snake. In: 2016 computing in cardiology conference (CinC). IEEE; 2016. p. 473–6.

[66] Dong S, Luo G, Sun G, Wang K, Zhang H. A combined multi-scale deep learning and random forests approach for direct left ventricular volumes estimation in 3d echocardiography. In: 2016 computing in cardiology conference (Cinc). IEEE; 2016. p. 889–92.

[67] Leclerc S, Smistad E, Grenier T, Lartizien C, Ostvik A, Espinosa F, et al. Deep learning applied to multi-structure segmentation in 2d echocardiography: a preliminary investigation of the required database size. In: 2018 IEEE international Ultrasonics symposium (IUS). IEEE; 2018. p. 1–4.

[68] Zyuzin V, Sergey P, Mukhtarov A, Chumarnaya T, Solovyova O, Bobkova A, et al. Identification of the left ventricle endocardial border on two-dimensional ultrasound images using the convolutional neural network unet. In: 2018 Ural symposium on biomedical engineering, radioelectronics and information technology (USBEREIT). IEEE; 2018. p. 76–8.

[69] Raynaud C, Langet H, Amzulescu MS, Saloux E, Bertrand H, Allain P, et al. Handcrafted features vs convnets in 2d echocardiographic images. In: 2017 IEEE 14th international symposium on biomedical imaging (ISBI 2017). IEEE; 2017. p. 1116–9.

[70] Jafari MH, Girgis H, Woudenberg N Van, Liao Z, Rohling R, Gin K, et al. Automatic biplane left ventricular ejection fraction estimation with mobile point-of-care ultrasound using multi-task learning and adversarial training. Int J Comput Assist Radiol Surg 2019;14(6):1027–37.

[71] Veni G, Moradi M, Bulu H, Narayan G, Syeda-Mahmood T. Echocardiography segmentation based on a shape-guided deformable model driven by a fully convolutional network prior. In: 2018 IEEE 15th international symposium on biomedical imaging (ISBI 2018). IEEE; 2018. p. 898–902.

[72] Dong S, Luo G, Wang K, Cao S, Li Q, Zhang H. A combined fully convolutional networks and deformable model for automatic left ventricle segmentation based on 3d echocardiography. Biomed Res Int 2018;2018.

[73] Ge R, Yang G, Chen Y, Luo L, Feng C, Zhang H, et al. Pv-lvnet: direct left ventricle multitype indices estimation from 2d echocardiograms of paired apical views with deep neural networks. Med Image Anal 2019;58:101554.

[74] Zyuzin V, Bobkova A, Porshnev S, Mukhtarov A, Bobkov V. The application of decision trees algorithm for selecting the area of the left ventricle on echocardiographic images. In: First international workshop on pattern recognition. vol. 10011. International Society for Optics and Photonics; 2016. 100110I.

[75] Bobkova A, Zyuzin V, Porshnev S, Bobkov V. Experience of using of machine learning methods to identify the left ventricle region in echocardiographic records. In: 2016 IEEE 10th international conference on application of information and communication technologies (AICT). IEEE; 2016. p. 1–5.

[76] Bobkov V, Bobkova A, Porshnev S, Zuzin V. The application of ensemble learning for delineation of the left ventricle on echocardiographic records. In: 2016 dynamics of systems, mechanisms and machines (dynamics). IEEE; 2016. p. 1–5.

[77] Belous G, Busch A, Rowlands D, Gao Y. Segmentation of the left ventricle in echocardiography using contextual shape model. In: 2016 international conference on digital image computing: Techniques and applications (DICTA). IEEE; 2016. p. 1–7.

[78] Bernier M, Jodoin P-M, Humbert O, Lalande A. Graph cut-based method for segmenting the left ventricle from mri or echocardiographic images. Comput Med Imaging Graph 2017;58:1–12.

[79] Narang A, Mor-Avi V, Prado A, Volpato V, Prater D, Tamborini G, et al. Machine learning based automated dynamic quantification of left heart chamber volumes. Eur Heart J Cardiovasc Imaging 2018;20(5):541–9.

[80] Volpato V, Mor-Avi V, Narang A, Prater D, Gonçalves A, Tamborini G, et al. Automated, machine learning-based, 3d echocardiographic quantification of left ventricular mass. Echocardiography 2019;36(2):312–9.

[81] Kusunose K, Haga A, Inoue M, Fukuda D, Yamada H, Sata M. Clinically feasible and accurate view classification of echocardiographic images using deep learning. Biomolecules 2020;10(5):665.

[82] Moradi S, Oghli MG, Alizadehasl A, Shiri I, Oveisi N, Oveisi M, et al. Mfp-unet: a novel deep learning based approach for left ventricle segmentation in echocardiography. Phys Med 2019;67:58–69.

[83] Li M, Wang C, Zhang H, Yang G. Mv-ran: multiview recurrent aggregation network for echocardiographic sequences segmentation and full cardiac cycle analysis. Comput Biol Med 2020;120:1–16. https://doi.org/10.1016/j.compbiomed.2020.103728. 103728.

[84] Ta K, Ahn SS, Lu A, Stendahl JC, Sinusas AJ, Duncan JS. A semi-supervised joint learning approach to left ventricular segmentation and motion tracking in echocardiography. In: 2020 IEEE 17th international symposium on biomedical imaging (ISBI). IEEE; 2020. p. 1734–7.

[85] Arafati A, Morisawa D, Avendi MR, Amini MR, Assadi RA, Jafarkhani H, et al. Generalizable fully automated multi-label segmentation of four-chamber view echocardiograms based on deep convolutional adversarial networks. J R Soc Interface 2020;17(169):20200267.

[86] Ahn SS, Ta K, Lu A, Stendahl JC, Sinusas AJ, Duncan JS. Unsupervised motion tracking of left ventricle in echocardiography. In: Medical imaging 2020: Ultrasonic imaging and tomography. vol. 11319. International Society for Optics and Photonics; 2020. 113190Z.

[87] Li M, Dong S, Gao Z, Feng C, Xiong H, Zheng W, et al. Unified model for interpreting multi-view echocardiographic sequences without temporal information. Appl Soft Comput 2020;88:106049.

[88] Sustersic T, Anic M, Filipovic N. Heart left ventricle segmentation in ultrasound images using deep learning. In: 2020 IEEE 20th Mediterranean Electrotechnical conference (MELECON). IEEE; 2020. p. 321–4.

[89] Hu Y, Guo L, Lei B, Mao M, Jin Z, Elazab A, et al. Fully automatic pediatric echocardiography segmentation using deep convolutional networks based on bisenet. In: 2019 41st annual international conference of the IEEE engineering in medicine and biology society (EMBC). IEEE; 2019. p. 6561–4.

[90] Dong S, Luo G, Tam C, Wang W, Wang K, Cao S, et al. Deep atlas network for efficient 3d left ventricle segmentation on echocardiography. Med Image Anal 2020;61:101638.

[91] Smistad E, Østvik A, Salte IM, Melichova D, Nguyen TM, Haugaa K, et al. Real-time automatic ejection fraction and foreshortening detection using deep learning. IEEE Trans Ultrason Ferroelec Freq Control 2020;67(12):2595–604. https://doi.org/10.1109/TUFFC.2020.2981037.

[92] Asch FM, Poilvert N, Abraham T, Jankowski M, Cleve J, Adams M, et al. Automated echocardiographic quantification of left ventricular ejection fraction without volume measurements using a machine learning algorithm mimicking a human expert. Circ Cardiovasc Imaging 2019;12(9):e009303.

[93] Leclerc S, Grenier T, Espinosa F, Bernard O. A fully automatic and multi-structural segmentation of the left ventricle and the myocardium on highly heterogeneous 2d echocardiographic data. In: 2017 IEEE international Ultrasonics symposium (IUS). IEEE; 2017. p. 1–4.

[94] Leclerc S, Smistad E, Pedrosa J, Østvik A, Cervenansky F, Espinosa F, et al. Deep learning for segmentation using an open large-scale dataset in 2d echocardiography. IEEE Trans Med Imaging 2019;38(9):2198–210. https://doi.org/10.1109/TMI.2019.2900516.

[95] Leclerc S, Smistad E, Grenier T, Lartizien C, Ostvik A, Cervenansky F, et al. Ru-net: A refining segmentation network for 2d echocardiography. In: 2019 IEEE international Ultrasonics symposium (IUS). IEEE; 2019. p. 1160–3.

[96] Smistad E, Salte IM, Østvik A, Leclerc S, Bernard O, Lovstakken L. Segmentation of apical long axis, four-and two-chamber views using deep neural networks. In: 2019 IEEE international Ultrasonics symposium (IUS). IEEE; 2019. p. 8–11.

[97] Leclerc S, Smistad E, Østvik A, Cervenansky F, Espinosa F, Espeland T, et al. Lu-net: a multi-stage attention network to improve the robustness of segmentation of left ventricular structures in 2d echocardiography. IEEE Trans Ultrason Ferroelec Freq Control 2020;67(12):2519–30. https://doi.org/10.1109/TUFFC.2020.3003403.

[98] Amer A, Ye X, Zolgharni M, Janan F. Resdunet: residual dilated unet for left ventricle segmentation from echocardiographic images. In: 2020 42nd annual international conference of the IEEE Engineering in Medicine & Biology Society (EMBC). IEEE; 2020. p. 2019–22.

[99] Zyuzin V, Mukhtarov A, Neustroev D, Chumarnaya T. Segmentation of 2d echocardiography images using residual blocks in u-net architectures. In: 2020 Ural Symposium on Biomedical Engineering, Radioelectronics and Information Technology (USBEREIT). IEEE; 2020. p. 499–502.

[100] Genovese D, Rashedi N, Weinert L, Narang A, Addetia K, Patel AR, et al. Machine learning–based three-dimensional echocardiographic quantification of right ventricular size and function: validation against cardiac magnetic resonance. J Am Soc Echocardiogr 2019;32(8):969–77. https://doi.org/10.1016/j.echo.2019.04.001.

[101] Ahmad A, Ibrahim Z, Sakr G, El-Bizri A, Masri L, Elhajj IH, et al. A comparison of artificial intelligence-based algorithms for the identification of patients with depressed right ventricular function from 2-dimentional echocardiography parameters and clinical features. Cardiovasc Diagnosis Ther 2020;10(4):859.

[102] Beecy AN, Bratt A, Yum B, Sultana R, Das M, Sherifi I, et al. Development of novel machine learning model for right ventricular quantification on echocardiography—a multimodality validation study. Echocardiography 2020;37(5):688–97.

[103] Bellavia D, Iacovoni A, Agnese V, Falletta C, Coronnello C, Pasta S, et al. Usefulness of regional right ventricular and right atrial strain for prediction of

early and late right ventricular failure following a left ventricular assist device implant: a machine learning approach. Int J Artif Organs 2020;43(5):297–314.
[104] Yuan B, Chitturi SR, Iyer G, Li N, Xu X, Zhan R, et al. Machine learning for cardiac ultrasound time series data. In: Medical imaging 2017: Biomedical applications in molecular, structural, and functional imaging. vol. 10137. International Society for Optics and Photonics; 2017. 101372D.
[105] Omar HA, Patra A, Domingos JS, Leeson P, Noblel AJ. Automated myocardial wall motion classification using handcrafted features vs a deep cnn-based mapping. In: 2018 40th annual international conference of the IEEE engineering in medicine and biology society (EMBC). IEEE; 2018. p. 3140–3.
[106] Dezaki FT, Liao Z, Luong C, Girgis H, Dhungel N, Abdi AH, et al. Cardiac phase detection in echocardiograms with densely gated recurrent neural networks and global extrema loss. IEEE Trans Med Imaging 2018;38(8):1821–32. https://doi.org/10.1109/TMI.2018.2888807.
[107] Kusunose K, Abe T, Haga A, Fukuda D, Yamada H, Harada M, et al. A deep learning approach for assessment of regional wall motion abnormality from echocardiographic images. JACC Cardiovasc Imaging 2019;13:374–81.
[108] Silva JF, Silva JM, Guerra A, Matos S, Costa C. Ejection fraction classification in transthoracic echocardiography using a deep learning approach. In: 2018 IEEE 31st international symposium on computer-based medical systems (CBMS). IEEE; 2018. p. 123–8.
[109] Zhong J, Liu P, Li S, Huang X, Zhang Q, Huang J, et al. A comparison of three-dimensional speckle tracking echocardiography parameters in predicting left ventricular remodeling. J Healthc Eng 2020;2020.
[110] Sabovčik F, Cauwenberghs N, Kouznetsov D, Haddad F, Alonso-Betanzos A, Vens C, et al. Applying machine learning to detect early stages of cardiac remodelling and dysfunction. Eur Heart J Cardiovasc Imaging 2020;00:1–10. https://doi.org/10.1093/ehjci/jeaa135.
[111] Mishra RK, Tison GH, Fang Q, Scherzer R, Whooley MA, Schiller NB. Association of machine learning–derived phenogroupings of echocardiographic variables with heart failure in stable coronary artery disease: the heart and soul study. J Am Soc Echocardiogr 2020;33(3):322–31.
[112] Kwon J-M, Jeon K-H, Kim HM, Kim MJ, Lim SM, Kim K-H, et al. Comparing the performance of artificial intelligence and conventional diagnosis criteria for detecting left ventricular hypertrophy using electrocardiography. EP Europace 2020;22(3):412–9.
[113] Ghorbani A, Ouyang D, Abid A, He B, Chen JH, Harrington RA, et al. Deep learning interpretation of echocardiograms. NPJ Digit Med 2020;3(1):1–10.
[114] Jian Z, Wang X, Zhang J, Wang X, Deng Y. Diagnosis of left ventricular hypertrophy using convolutional neural network. BMC Med Inform Decis Mak 2020;20(1):1–12.
[115] Hedman ÅK, Hage C, Sharma A, Brosnan MJ, Buckbinder L, Gan L-M, et al. Identification of novel pheno-groups in heart failure with preserved ejection fraction using machine learning. Heart 2020;106(5):342–9.
[116] Howard JP, Tan J, Shun-Shin MJ, Mahdi D, Nowbar AN, Arnold AD, et al. Improving ultrasound video classification: an evaluation of novel deep learning methods in echocardiography. J. Med Artif Intell 2020;3.
[117] Liao Z, Girgis H, Abdi A, Vaseli H, Hetherington J, Rohling R, et al. On modelling label uncertainty in deep neural networks: automatic estimation of intra-observer variability in 2d echocardiography quality assessment. IEEE Trans Med Imaging 2019;39(6):1868–83.
[118] Kagiyama N, Shrestha S, Cho JS, Khalil M, Singh Y, Challa A, et al. A low-cost texture-based pipeline for predicting myocardial tissue remodeling and fibrosis using cardiac ultrasound. EBioMedicine 2020;54:102726.
[119] Chandra V, Sarkar PG, Singh V. Mitral valve leaflet tracking in echocardiography using custom yolo3. Procedia Computer Science 2020;171:820–8.
[120] Samad MD, Ulloa A, Wehner GJ, Jing L, Hartzel D, Good CW, et al. Predicting survival from large echocardiography and electronic health record datasets: optimization with machine learning. JACC Cardiovasc Imaging 2018:2641.
[121] Raghavendra U, Fujita H, Gudigar A, Shetty R, Nayak K, Pai U, et al. Automated technique for coronary artery disease characterization and classification using dd-dtdwt in ultrasound images. Biomed Signal Process Control 2018;40:324–34.
[122] Raghavendra U, Acharya UR, Gudigar A, Shetty R, Krishnananda N, Pai U, et al. Automated screening of congestive heart failure using variational mode decomposition and texture features extracted from ultrasound images. Neural Comput Appl 2017;28(10):2869–78.
[123] Moghaddasi H, Nourian S. Automatic assessment of mitral regurgitation severity based on extensive textural features on 2d echocardiography videos. Comput Biol Med 2016;73:47–55.
[124] Smistad E, Østvik A, Salte IM, Leclerc S, Bernard O, Lovstakken L. Fully automatic real-time ejection fraction and mapse measurements in 2d echocardiography using deep neural networks. In: 2018 IEEE international ultrasonics symposium (IUS). IEEE; 2018. p. 1–4.
[125] bin Ahmad Nizar MH, Chan CK, Yusof AKM, Khalil A, Lai KW. Detection of aortic valve from echocardiography in real-time using convolutional neural network. In: 2018 IEEE-EMBS conference on biomedical engineering and sciences (IECBES). IEEE; 2018. p. 91–5.
[126] Pereira F, Bueno A, Rodriguez A, Perrin D, Marx G, Cardinale M, et al. Automated detection of coarctation of aorta in neonates from two-dimensional echocardiograms. J Med Imaging 2017;4(1):014502.
[127] Khalil A, Faisal A, Lai KW, Ng SC, Liew YM. 2d to 3d fusion of echocardiography and cardiac ct for tavr and tavi image guidance. Med Biol Eng Comput 2017;55(8):1317–26.
[128] Otani K, Nakazono A, Salgo IS, Lang RM, Takeuchi M. Three-dimensional echocardiographic assessment of left heart chamber size and function with fully automated quantification software in patients with atrial fibrillation. J Am Soc Echocardiogr 2016;29(10):955–65.
[129] Borkar S, Annadate M. Supervised machine learning algorithm for detection of cardiac disorders. In: 2018 fourth international conference on computing communication control and automation (ICCUBEA). IEEE; 2018. p. 1–4.
[130] Lu A, Dehghan E, Veni G, Moradi M, Syeda-Mahmood T. Detecting anomalies from echocardiography using multi-view regression of clinical measurements. In: 2018 IEEE 15th international symposium on biomedical imaging (ISBI 2018). IEEE; 2018. p. 1504–8.
[131] Lei J, Wang YG, Bhatta L, Ahmed J, Fan D, Wang J, et al. Ventricular geometry–regularized qrsd predicts cardiac resynchronization therapy response: machine learning from crosstalk between electrocardiography and echocardiography. Int J Cardiovasc Imaging 2019:1–9.
[132] Gifani P, Behnam H, Haddadi F, Sani ZA, Gifani P. Echocardiography noise reduction using sparse representation. Comput Elec Eng 2016;53:301–18.
[133] Punithakumar K, Hareendranathan AR, McNulty A, Biamonte M, He A, Noga M, et al. Multiview 3-d echocardiography fusion with breath-hold position tracking using an optical tracking system. Ultrasound Med Biol 2016;42(8):1998–2009.
[134] Abdi AH, Luong C, Tsang T, Allan G, Nouranian S, Jue J, et al. Automatic quality assessment of echocardiograms using convolutional neural networks: feasibility on the apical four-chamber view. IEEE Trans Med Imaging 2017;36(6):1221–30.
[135] Diller G-P, Lammers AE, Babu-Narayan S, Li W, Radke RM, Baumgartner H, et al. Denoising and artefact removal for transthoracic echocardiographic imaging in congenital heart disease: utility of diagnosis specific deep learning algorithms. Int J Cardiovasc Imaging 2019:1–8.
[136] Wu H, Huynh TT, Souvenir R. Echocardiogram enhancement using supervised manifold denoising. Med Image Anal 2015;24(1):41–51.
[137] Girum KB, Créhange G, Hussain R, Lalande A. Fast interactive medical image segmentation with weakly supervised deep learning method. Int J Comput Assist Radiol Surg 2020;15(9):1437–44.
[138] Teng L, Fu Z, Ma Q, Yao Y, Zhang B, Zhu K, et al. Interactive echocardiography translation using few-shot gan transfer learning. Comput Math Methods Med 2020;2020.
[139] D'hooge J, Fraser AG. Learning about machine learning to create a self-driving echocardiographic laboratory: technical considerations. 2018.
[140] Arabasadi Z, Alizadehsani R, Roshanzamir M, Moosaei H, Yarifard AA. Computer aided decision making for heart disease detection using hybrid neural network-genetic algorithm. Comput Methods Prog Biomed 2017;141:19–26.